A comparison of the results obtained with NaCl, KCl, and KBr is interesting. Even in the purest NaCl crystals colored and kept in the dark, σ_c/σ_n is considerably suppressed in the temperature range 100–500°C, and excess conductivity due to F-aggregate centers or colloids is not observed.[11] The excess conductivity due to R, M, and colloids is significant in KCl if crystals are of high purity. The excess conductivity due to F-aggregate centers in the purest KBr crystals is larger by a factor of ~ 3 as compared to KCl crystals. The 180°C peak observed in KBr in the dark is not observed in KCl crystals. The background divalent cation impurity concentration (estimated from the conductivity data) in the best crystals used by us are 10^{-5} in NaCl, 10^{-6} in KCl, and better than 10^{-8} molar fraction in KBr. We believe that the differences in the behavior of the NaCl, KCl, or KBr are related to the differences in the concentration of background impurity in the crystals. KCl and KBr crystals containing large background impurity concentration behave like NaCl crystals.

ACKNOWLEDGMENT

We are deeply indebted to Dr. G. D. Sootha for many useful discussions and for his help in preparing this manuscript.

PHYSICAL REVIEW VOLUME 181, NUMBER 3 15 MAY 1969

Normal Modes of a Semi-Infinite Ionic Crystal

S. Y. Tong and A. A. Maradudin
Department of Physics, University of California, Irvine, California 92664
(Received 19 July 1968; revised manuscript received 13 December 1968)

The normal modes of a semi-infinite ionic crystal bounded by a pair of (100) faces normal to the z direction but infinite in the x and y directions have been determined by a combination of analytical and numerical methods. Cyclic boundary conditions are imposed on the displacements along the x and y directions, but the presence of a pair of free surfaces is correctly incorporated into both the short-range and the long-range Coulomb contributions to the dynamical matrix. The latter contribution is made rapidly convergent by a modified Bessel-function transformation. The $6L\times 6L$ (L=number of atomic planes for the slab) eigenvalue equation for the normal-mode frequencies is solved numerically for general values of the wave vector throughout the two-dimensional first Brilluion zone. The two lowest-frequency modes are Rayleigh waves, whose degeneracy is slightly split by the presence of a pair of free surfaces. Optical surface modes are found whose limiting frequencies at infinite wavelength differ from those of the bulk LO and TO modes. The contribution to infrared absorption at infinite wavelength of the optical surface modes have been calculated and the effects of relaxing the intraplanar lattice parameter and the interplanar separations to minimize the potential energy of the slab have also been determined.

I. INTRODUCTION

THE problem of determining the normal modes and their frequencies of finite or semi-infinite specimens of ionic crystals has received a good deal of theoretical attention in recent years.[1–7] Particular attention has been given to the determination of the frequencies of the long-wavelength optical modes which play a central role in determining the optical properties of ionic crystals at infrared frequencies. Inasmuch as the long-range Coulomb forces between ions make a significant contribution to the frequencies of the long-wavelength optical modes through the macroscopic fields to which they give rise, these frequencies are sensitive to the size and shape of the crystal specimens.

The limiting optical frequencies of a finite spherical crystal of the rocksalt structure were studied by Maradudin and Weiss,[2] neglecting retardation effects. These authors found that in the long-wavelength limit the frequencies of the longitudinal optical (LO) and transverse optical (TO) modes are equal, in contrast with the result obtained for infinitely extended crystals, in which these frequencies obey the Lyddane-Sachs-Teller[8] relation, $\omega_{LO}/\omega_{TO}=(\epsilon_0/\epsilon_\infty)^{1/2}\neq 1$, where ϵ_0 and ϵ_∞ are the static and high-frequency dielectric constants, respectively.[1] More recently, Fuchs and Kliewer[4] have examined the optical modes of an ionic crystal slab extending to infinity in the two lateral directions and of finite thickness. Neglecting retardation they found in this case that as the wave vector $\mathbf{k}\rightarrow 0$, the frequencies of the LO and TO modes are those of the infinitely extended crystal, and satisfy the Lyddane-Sachs-Teller

[1] H. B. Rosenstock, Phys. Rev. **121**, 416 (1961).
[2] A. A. Maradudin and G. H. Weiss, Phys. Rev. **123**, 1968 (1961).
[3] T. H. K. Barron, Phys. Rev. **123**, 1995 (1961).
[4] R. Fuchs and K. L. Kliewer, Phys. Rev. **140**, A2076 (1965); K. L. Kliewer and R. Fuchs, *ibid.* **144**, 495 (1966); **150**, 573 (1966).
[5] R. Englman and R. Ruppin, Phys. Rev. Letters **16**, 898 (1966).
[6] A. A. Lucas, Phys. Rev. **162**, 801 (1967).
[7] A. A. Lucas (unpublished).
[8] R. H. Lyddane, R. G. Sachs, and E. Teller, Phys. Rev. **59**, 673 (1941).

relation. The difference between this result and that of Maradudin and Weiss is due primarily to the difference between the deplorizing fields associated with a sphere and with a slab. However, in addition to the long-wavelength optical modes of the infinitely extended crystal, Fuchs and Kliewer found that the slab possesses two branches of surface optical modes as well. These are normal modes which are wavelike in directions parallel to the free surfaces of the slab, but in which the atomic displacement amplitudes decay exponentially with increasing distance into the slab from the free surfaces. Unlike the case of Rayleigh surface modes,[9] which are acoustic surface modes, the frequencies of surface optical modes tend to nonzero limits as the components of their wave vectors parallel to the free surface, k_x and k_y, tend to zero, and are characterized by the motion of the constituent sublattices against each other rather than in parallel, as is the case for Rayleigh waves. Fuchs and Kliewer found that at the point $k_x=k_y=0$, the two surface modes become one "longitudinal" and one "transverse" in nature and their frequencies approach those of the limiting LO and TO frequencies of the infinitely extended crystal. The two surface modes have the property that the displacement amplitudes do not decay with increasing distance into the crystal at $k_x=k_y=0$.

In their work, Fuchs and Kliewer approximated two-dimensional lattice sums, which give the force exerted on an ion by other ions in a certain layer of the slab through their Coulomb interactions by converting them into integrals. As we shall see in Sec. IV, this kind of approximation is not valid for determining the frequencies of modes of very long wavelengths. Also, they did not include any correction to the short-range forces acting on ions in the crystal surfaces due to the smaller numbers of neighbors such ions have.

Corrections to the short-range forces from this source were included in a recent work by Lucas.[7] He approximated a semi-infinite slab of N layers of ions by a double chain of N ions each, and calculated the normal-mode frequencies of the double chain for the special case $k_x=k_y=0$. Coulomb interactions between nearest-neighbor layers were taken into account only. He found two nearly degenerate TO surface modes; the frequencies of both of these modes lie below the limitingTO frequency of the infinitely extended crystal. Also, unlike what Fuchs and Kliewer obtained, these surface modes have displacement amplitudes that attenuate exponentially as a function of increasing distance into the crystal from the free surfaces, even at $k_x=k_y=0$.

It is felt that the discrepancies between the two works may have arisen from the different approximation methods employed in each case and that a method of higher accuracy is required to get the complete picture for the vibrational modes of the slab. In this paper, we study the vibrations of a slab of finite thickness by a method that gives us both the acoustic and optical normal modes and their frequencies for arbitrary wave vectors in the irreducible element of the two-dimensional Brillouin zone. Both the Rayleigh waves and the surface optical modes are found. The presence of a pair of free surfaces is correctly incorporated into the short-range and the long-range Coulomb contributions to the dynamical matrix. The contributions from Coulomb interactions between all the layers in the slab are included. We find at certain regions in the Brillouin zone that these Coulomb interactions between the layers are slow varying and long-ranged. In these regions, "surface" effects penetrate deeply into the crystal slab. It is then no longer a valid approximation to include Coulomb interactions between nearest-neighbor layers alone. The effects due to relaxation of the ionic layers near the free surfaces are also included. Our results for the surface optical modes differ significantly from those of Fuchs and Kliewer,[4] and at the point $k_x=k_y=0$, our results agree in part with those obtained by Lucas.[7]

In Sec. VI of this paper, the frequency distribution curve of the slab is compared with that of an infinitely extended crystal with cyclic boundary conditions. Peaks in the difference curve appear at where the surface modes are located. In Sec. VII, the contribution of the surface optical modes to infrared absorption is calculated.

II. EQUATIONS OF MOTION OF A VIBRATION SLAB

We consider a crystal slab consisting of a finite number of layers, each layer perpendicular to the z axis (the [001] direction), and extending to infinity in the x and y directions. The position vector of the κth ion in the lth unit cell is given by

$$\mathbf{x}(l\kappa)=\mathbf{x}(l)+\mathbf{x}(\kappa)\,, \tag{2.1}$$

where $\mathbf{x}(l)$ is the position vector of the lth unit cell and $\mathbf{x}(\kappa)$ is the position vector of the κth ion in any unit cell.

The equations of motion of the lattice are[10]

$$M_\kappa \ddot{u}_\alpha(l\kappa)=-\sum_{l'\kappa'\beta}\Phi_{\alpha\beta}(l\kappa;\,l'\kappa')u_\beta(l'\kappa')\,, \tag{2.2}$$

where M_κ is the mass of the κth kind of ion, $u_\alpha(l\kappa)$ is the α-Cartesian component of the displacement of the ion $(l\kappa)$, and $\Phi_{\alpha\beta}(l\kappa;\,l'\kappa')$ are the atomic force constants. With the substitution

$$u_\alpha(l\kappa)=[v_\alpha(l\kappa)/M_\kappa{}^{1/2}]e^{-i\omega t}\,,$$

Eq. (2.2) becomes

$$\omega^2 v_\alpha(l\kappa)=\sum_{l'\kappa'\beta}\frac{\Phi_{\alpha\beta}(l\kappa;\,l'\kappa')}{(M_\kappa M_{\kappa'})^{1/2}}v_\beta(l'\kappa')\,. \tag{2.3}$$

[9] Lord Rayleigh, Proc. London Math. Soc. **17**, 4 (1885); G. C. Benson, P. I. Freeman, and E. Dempsey, J. Chem. Phys. **39**, 302 (1963).

[10] A. A. Maradudin, E. W. Montroll, and G. W. Weiss, *Theory of Lattice Dynamics in the Harmonic Approximation* (Academic Press Inc., New York, 1963).

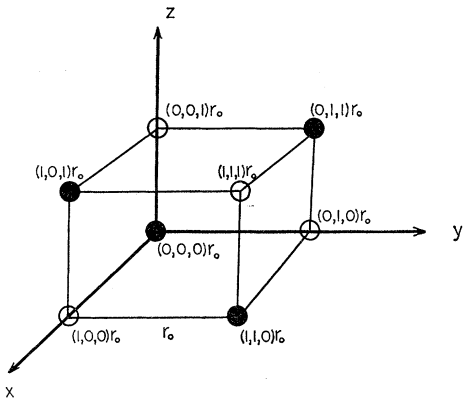

FIG. 1. Diatomic cubic lattice with the (+) ions located at $r_0(l_1,l_2,l_3)$, where $l_1+l_2+l_3$=even integer, and the (−) ions at $r_0(l_1,l_2,l_3)$, where $l_1+l_2+l_3$=odd integer.

We assume the crystal to have the rocksalt structure. In this case κ denotes either a (+) ion or a (−) ion. We can eliminate the sum over κ' in Eq. (2.3) by noticing that if we assume the origin of coordinates (0,0,0) to be occupied by a (+) ion, then

$$\mathbf{x}(l_+)=r_0(l_1,l_2,l_3)\,,\quad l_1+l_2+l_3=\text{even}$$
$$\mathbf{x}(l_-)=r_0(l_1,l_3,l_2)\,,\quad l_1+l_2+l_3=\text{odd}$$

where r_0 is the distance between nearest-neighbor ions (see Fig. 1).

Equation (2.3) then separates into

$$\omega^2 v_\alpha{}^{(+)}(l_1l_2l_3)=\sum_\beta\Bigg[\frac{1}{M_+}\sum_{l_1'l_2'l_3'}^{\text{even}}\Phi_{\alpha\beta}{}^{(+,+)}(l_1l_2l_3;\,l_1'l_2'l_3')\times V_\beta{}^{(+)}(l_1'l_2'l_3')+\frac{1}{(M_+M_-)^{1/2}}\sum_{l_1'l_2'l_3'}^{\text{odd}}\Phi_{\alpha\beta}{}^{(+,-)}(l_1l_2l_3;\,l_1'l_2'l_3')v_\beta{}^{(-)}(l_1'l_2'l_3)\Bigg],$$
$$l_1+l_2+l_3=\text{even}\quad(2.4a)$$

and

$$\omega^2 v_\alpha{}^{(-)}(l_1l_2l_3)=\sum_\beta\Bigg[\frac{1}{(M_+M_-)^{1/2}}\sum_{l_1'l_2'l_3'}^{\text{even}}\Phi_{\alpha\beta}{}^{(-,+)}(l_1l_2l_3;\,l_1'l_2'l_3')v_\beta{}^{(+)}(l_1'l_2'l_3')+\frac{1}{M_-}\sum_{l_1'l_2'l_3'}^{\text{odd}}\Phi_{\alpha\beta}{}^{(-,-)}(l_1l_2l_3;\,l_1'l_2'l_3')v_\beta{}^{(-)}(l_1'l_2'l_3)\Bigg],$$
$$l_1+l_2+l_3=\text{odd}\quad(2.4b)$$

where the word even or odd appearing above the triple sums denotes the restrictions $l_1'+l_2'+l_3'$=even or $l_1'+l_2'+l_3'$=odd, respectively, on the summation variables.

Due to the existence of the pair of free surfaces perpendicular to the z direction, we can assume wavelike solutions satisfying periodic boundary conditions in the x and y directions. We therefore write $v_\alpha{}^{(+)}(l_1l_2l_3)$ as the product of a wavelike function of l_1 and l_2 and an unknown function of l_3:

$$v_\alpha{}^{(+e)}(l_1l_2l_3)=\exp(il_1\phi_1+il_2\phi_2)\zeta_\alpha{}^{(+e)}(l_3)\,,\quad l_3\text{ even},\ l_1+l_2\text{ even}$$

and

$$v_\alpha{}^{(+o)}(l_1l_2l_3)=\exp(il_1\phi_1+il_2\phi_2)\zeta_\alpha{}^{(+o)}(l_3),\quad l_3\text{ odd},\ l_1+l_2\text{ odd}\quad(2.5a)$$

where $\phi_1=k_xr_0$ and $\phi_2=k_yr_0$, and the symbol (e) or (o) denotes that l_3 labels an even or an odd layer, respectively. Similarly, we write $v_\alpha{}^{(-)}(l_1l_2l_3)$ as the product of two factors:

$$v_\alpha{}^{(-e)}(l_1l_2l_3)=\exp(il_1\phi_1+il_2\phi_2)\zeta_\alpha{}^{(-e)}(l_3)\,,\quad l_3\text{ even},\ l_1+l_2\text{ odd}$$

and

$$v_\alpha{}^{(-o)}(l_1l_2l_3)=\exp(il_1\phi_1+il_2\phi_2)\zeta_\alpha{}^{(-o)}(l_3)\,,\quad l_3\text{ odd},\ l_1+l_2\text{ even}.\quad(2.5b)$$

Using Eqs. (2.5a) and (2.5b), we can rewrite Eqs. (2.4a) and (2.4b) as a set of four equations with the general form

$$\omega^2\zeta_\alpha{}^{(\kappa p)}(l_3)=\sum_{l_3'\beta}\sum_{\kappa'p'}D_{\alpha\beta}{}^{(\kappa p;\kappa'p')}(\phi_1\phi_2;\,l_3l_3')\zeta_\beta{}^{(\kappa'p')}(l_3')\,,\qquad\kappa,\kappa'=(+)\text{ or }(-),\ p,p'=(e)\text{ or }(o),\quad(2.6)$$

where

$$D_{\alpha\beta}{}^{(\kappa p;\kappa'p')}(\phi_1\phi_2;\,l_3l_3')=\frac{1}{(M_\kappa M_{\kappa'})^{1/2}}\sum_{l_1'l_2'}^{(r)}\Phi_{\alpha\beta}{}^{(\kappa p;\kappa'p')}(l_1l_2l_3;\,l_1'l_2'l_3')\times\exp[i(l_1'-l_1)\phi_1+i(l_2'-l_2)\phi_2].\quad(2.7)$$

The (r) on the summation symbol denotes the restriction on the double sum over l_1' and l_2' that $l_1'+l_2'$ is an even integer or an odd integer according to whether the product of the parities of κ' and p' is even or odd [the parity of $\kappa'=(+)$ is regarded as even; that of $\kappa'=(-)$ as odd].

Equation (2.6) is a $6N\times6N$ (N=number of layers in the slab) matrix equation with the squares of the normal-mode frequencies as its eigenvalues.

In the remainder of this work we assume that each pair of ions interacts through a potential function of $\phi_{\kappa\kappa'}(r)$, which depends only on the magnitude of their separation, r. In this case the atomic force constants $\Phi_{\alpha\beta}(l\kappa;\,l'\kappa')$ take the form

$$\Phi_{\alpha\beta}(l\kappa;\,l'\kappa')=-\frac{\partial^2}{\partial x_\alpha\partial x_\beta}\phi_{\kappa\kappa'}(r)\big|_{r=\mathbf{x}(l\kappa)-\mathbf{x}(l'\kappa')}=\Phi_{\alpha\beta}(l'\kappa';\,l\kappa).\quad(2.8)$$

Since the potential function depends only on the relative distance between the ions at the sites labeled by (l_1,l_2,l_3) and (l_1',l_2',l_3'), $\Phi_{\alpha\beta}(l_1l_2l_3;\, l_1'l_2'l_3')$ is a function of l_1, l_2, l_1', l_2' only through the difference (l_1-l_1') and (l_2-l_2'). Introducing the notation $\bar{l}_1=l_1-l_1'$ and $\bar{l}_2=l_2-l_2'$, we can rewrite Eq. (2.7) as

$$D_{\alpha\beta}{}^{(\kappa p;\kappa' p')}(\phi_1\phi_2;\, l_3l_3') = \frac{1}{(M_\kappa M_{\kappa'})^{1/2}} \sum_{\bar{l}_1\bar{l}_2}^{(r)} \Phi_{\alpha\beta}{}^{(\kappa p;\kappa' p')}(\bar{l}_1\bar{l}_2;\, l_3l_3') \times \exp(-i\bar{l}_1\phi_1 - i\bar{l}_2\phi_2), \quad (2.9)$$

where $\bar{l}_1+\bar{l}_2$ is now an even or an odd integer according to whether the product of the parities of κ, p, κ', and p' is even or odd, respectively.

III. MATRIX ELEMENTS FOR THE SHORT-RANGE INTERACTIONS

The dynamical matrix $D_{\alpha\beta}{}^{(\kappa p;\kappa' p')}(\phi_1\phi_2;\, l_3l_3')$ defined by Eq. (2.9) can be divided into two parts, a part $D_{\alpha\beta}{}^{c(\kappa p;\kappa' p')}(\phi_1\phi_2;\, l_3l_3')$ corresponding to the Coulomb interactions between the ions and a part $D_{\alpha\beta}{}^{s(\kappa p;\kappa' p')}(\phi_1\phi_2;\, l_3l_3')$ corresponding to the short-range interactions.

Let us define two constants A and B[11] by

$$A = \frac{4r_0{}^3}{e^2}\frac{d^2V(r)}{dr^2}\bigg|_{r=r_0}, \qquad B = \frac{4r_0{}^2}{e^2}\frac{dV(r)}{dr}\bigg|_{r=r_0}, \quad (3.1)$$

where $V(r)$ is the nearest-neighbor interaction potential. For nearest-neighbor short-range interactions, the matrices $D_{\alpha\beta}{}^{s(\kappa p;\kappa' p')}(\phi_1\phi_2;\, l_3l_3')$ are all diagonal. For a slab with N layers, their explicit forms are

Case (i): $\kappa=\kappa'$, $p=p'$,

$$D_{\alpha\beta}{}^{s(\kappa p;\kappa p)}(\phi_1\phi_2;\, l_3l_3') = (e^2/M_\kappa r_0{}^3)\delta_{l_3,l_3'}\delta_{\alpha\beta}(\tfrac{1}{2}A+B), \quad \text{for } l_3\neq 1 \text{ or } N \quad (3.2)$$

$$D_{xx}{}^{s(\kappa p;\kappa p)}(\phi_1\phi_2;\, l_3l_3') = D_{yy}{}^{s(\kappa p;\kappa p)}(\phi_1\phi_2;\, l_3l_3') = (e^2/M_\kappa r_0{}^3)\delta_{l_3,l_3'}(\tfrac{1}{2}A+\tfrac{3}{4}B), \quad \text{for } l_3=1 \text{ or } N \quad (3.3a)$$

$$D_{zz}{}^{s(\kappa p;\kappa p)}(\phi_1\phi_2;\, l_3l_3') = (e^2/M_\kappa r_0{}^3)\delta_{l_3,l_3'}(\tfrac{1}{4}A+B), \quad \text{for } l_3=1 \text{ or } N; \quad (3.3b)$$

Case (ii): $\kappa\neq\kappa'$, $p=p'$,

$$D_{xx}{}^{s(\kappa p;\kappa' p)}(\phi_1\phi_2;\, l_3,l_3') = -\frac{e^2}{(M_\kappa M_{\kappa'})^{1/2}r_0{}^3}\delta_{l_3,l_3'}(\tfrac{1}{2}A\cos\phi_1+\tfrac{1}{2}B\cos\phi_2),$$

$$D_{yy}{}^{s(\kappa p;\kappa' p)}(\phi_1\phi_2;\, l_3l_3') = -\frac{e^2}{(M_\kappa M_{\kappa'})^{1/2}r_0{}^3}\delta_{l_3,l_3'}(\tfrac{1}{2}B\cos\phi_1+\tfrac{1}{2}A\cos\phi_2),$$

$$D_{zz}{}^{s(\kappa p;\kappa' p)}(\phi_1\phi_2;\, l_3l_3') = -\frac{e^2}{(M_\kappa M_{\kappa'})^{1/2}r_0{}^3}\delta_{l_3,l_3'}[\tfrac{1}{2}B(\cos\phi_1+\cos\phi_2)]; \quad (3.4)$$

Case (iii): $\kappa\neq\kappa'$, $p\neq p'$

$$D_{\alpha\beta}{}^{s(\kappa p;\kappa p')}(\phi_1\phi_2;\, l_3l_3') = 0; \quad (3.5)$$

Case (iv): $\kappa\neq\kappa'$, $p\neq p'$,

$$D_{xx}{}^{s(\kappa p;\kappa' p')}(\phi_1\phi_2;\, l_3l_3') = D_{yy}{}^{s(\kappa p;\kappa' p')}(\phi_1\phi_2;\, l_3l_3') = -\frac{e^2}{(M_\kappa M_{\kappa'})^{1/2}r_0{}^3} \times [\tfrac{1}{4}B(\delta_{l_3,l_3'+1}+\delta_{l_3,l_3'-1})], \quad (3.6)$$

$$D_{zz}{}^{s(\kappa p;\kappa' p')}(\phi_1\phi_2;\, l_3l_3') = -\frac{e^2}{(M_\kappa M_{\kappa'})^{1/2}r_0{}^3}\tfrac{1}{4}A(\delta_{l_3,l_3'+1}+\delta_{l_3,l_3'-1}).$$

Notice that for any κ, κ' and p, p', the relation

$$D_{\alpha\beta}{}^{s(\kappa p;\kappa' p')}(\phi_1\phi_2;\, l_3l_3') = D_{\alpha\beta}{}^{s(\kappa' p';\kappa p)}(\phi_1\phi_2;\, l_3l_3')$$

always holds.

Of the above expressions, only (3.4) depends on the values of ϕ_1 and ϕ_2. In the limit as $\phi_1=\phi_2\to 0$, the above expressions become the same as those given by Fuchs and Kliewer,[4] who worked in the long-wavelength limit.

However, they have neglected the changes in these coefficients which occur at the surface layers, given here in Eqs. (3.3a) and (3.3b). Instead, they used the bulk expression (3.2) for all layers in the slab.

In Appendix A, the expressions for $D_{\alpha\beta}{}^{s(\kappa p;\kappa' p')}(\phi_1\phi_2;\, l_3l_3')$ for nearest and next-nearest-neighbor short-range forces are also given.

IV. MATRIX ELEMENTS FOR THE COULOMB INTERACTIONS BETWEEN IONS

The Coulomb contribution to $D_{\alpha\beta}{}^{(\kappa p;\kappa' p')}(\phi_1\phi_2;\, l_3l_3')$ defined by Eq. (2.9) is

$$D_{\alpha\beta}{}^{c(\kappa p;\kappa' p')}(\phi_1\phi_2;\, l_3l_3') = -\frac{e_\kappa e_{\kappa'}}{(M_\kappa M_{\kappa'})^{1/2}r_0{}^3} \times \sum_{\bar{l}_1\bar{l}_2}^{(r)} \frac{\exp(-i\bar{l}_1\phi_1 - i\bar{l}_2\phi_2)}{(\bar{l}_1{}^2+\bar{l}_2{}^2+\bar{l}_3{}^2)^{5/2}}[3\bar{l}_\alpha\bar{l}_\beta - \delta_{\alpha\beta}(\bar{l}_1{}^2+\bar{l}_2{}^2+\bar{l}_3{}^2)] = D_{\alpha\beta}{}^{c(\kappa' p';\kappa p)}(\phi_1\phi_2;\, l_3l_3'), \quad (4.1)$$

where e_κ is the charge of the κth ion, and $\bar{l}_3=l_3-l_3'$. As it stands, the lattice sum in Eq. (4.1) is slowly conver-

[11] E. W. Kellermann, Phil. Trans. Roy. Soc. London **A238**, 513 (1940).

gent, and must be transformed into a much more rapidly convergent sum before its numerical evaluation becomes feasible. We have carried out such a transformation using a method due originally to Mackenzie.[12] For illustration, we work out here the expression for $D_{\alpha\beta}{}^{c(\kappa p;\kappa' p')}(\phi_1\phi_2; l_3 l_3')$ for the case $\kappa=\kappa'$, $p=p'$.

From Eq. (4.1) we find that

$$D_{xx}{}^{c(\kappa p;\kappa p)}(\phi_1\phi_2; l_3 l_3') = -\frac{e^2}{M_\kappa r_0{}^3}\sum_{\substack{\bar{l}_1=-\infty\\ \bar{l}_1+\bar{l}_2=\text{even}}}^{\infty}\sum_{\bar{l}_2=-\infty}^{\infty}\frac{\exp(-i\bar{l}_1\phi_1-i\bar{l}_2\phi_2)}{(\bar{l}_1{}^2+\bar{l}_2{}^2+\bar{l}_3{}^2)^{5/2}} \times(2\bar{l}_1{}^2-\bar{l}_2{}^2-\bar{l}_3{}^2). \quad (4.2)$$

Let us for the moment consider the case when $l_3\neq l_3'$. We make use of the integral representation

$$\frac{1}{|\mathbf{r}|^s}=\frac{1}{T(\frac{1}{2}s)}\int_0^\infty dt\, t^{s/2-1}e^{-r^2t}$$

to rewrite Eq. (4.2) in the form

$$D_{xx}{}^{c(\kappa p;\kappa p)}(\phi_1\phi_2; l_3 l_3') = -\frac{e^2}{M_\kappa r_0{}^3}\frac{1}{T(\frac{5}{2})} \times\sum_{\substack{\bar{l}_1=-\infty\\ \bar{l}_1+\bar{l}_2=\text{even}}}^{\infty}\sum_{\bar{l}_2=-\infty}^{\infty}\int_0^\infty t^{3/2}dt\exp[-t(\bar{l}_1{}^2+\bar{l}_2{}^2+\bar{l}_3{}^2)] \times\exp(-i\bar{l}_1\phi_1-i\bar{l}_2\phi_2)(2\bar{l}_1{}^2-\bar{l}_2{}^2-\bar{l}_3{}^2). \quad (4.3)$$

The restriction $\bar{l}_1+\bar{l}_2=$ even means that either $\bar{l}_1$ and $\bar{l}_2$ are both even or that they are both odd. We can thus break the sum in Eq. (4.3) into two parts:

$$D_{xx}{}^{c(\kappa p;\kappa p)}(\phi_1\phi_2; l_3 l_3') = -\frac{e^2}{M_\kappa r_0{}^3}\frac{1}{T(\frac{5}{2})}(F_1+F_2), \quad (4.4)$$

where

$$F_1=\sum_{m=\infty}^{\infty}\sum_{n=\infty}^{\infty}\int_0^\infty t^{3/2}e^{-l_3{}^2t}dt \times\exp(-4m^2t-2im\phi_1-4n^2t-2in\phi_2) \times(8m^2-4n^2-\bar{l}_3{}^2) \quad (4.5a)$$

and

$$F_2=\sum_{m=\infty}^{\infty}\sum_{n=\infty}^{\infty}\int_0^\infty t^{3/2}dt\, e^{-l_3{}^2t}\exp[-4(m-\tfrac{1}{2})^2t -2i(m-\tfrac{1}{2})\phi_1-4(n-\tfrac{1}{2})^2t-2i(n-\tfrac{1}{2})\phi_2] \times[8(m-\tfrac{1}{2})^2-4(n-\tfrac{1}{2})^2-\bar{l}_3{}^2]. \quad (4.5b)$$

We convert the sums over m and n in Eqs. (4.5a) and (4.5b) into more convenient forms by the use of Poisson's summation formulas,[13]

$$\sum_{m=-\infty}^{\infty}\exp(-4m^2t-2im\phi) =\left(\frac{\pi}{4t}\right)^{1/2}\sum_{G=-\infty}^{\infty}e^{-(\phi+\pi G)^2/4t}, \quad (4.5c)$$

$$\sum_{m=-\infty}^{\infty}\exp[-4(m-\tfrac{1}{2})^2t-2i(m-\tfrac{1}{2})\phi] =\left(\frac{\pi}{4t}\right)^{1/2}\sum_{G=-\infty}^{\infty}(-1)^G e^{-(\phi+\pi G)^2/4t}. \quad (4.5d)$$

Then

$$F_1+F_2=\frac{\pi}{4}\sum_{G=-\infty}^{\infty}\sum_{H=-\infty}^{\infty}\int_0^\infty t^{1/2}dt\, e^{-l_3{}^2t} \times\exp\left(-\frac{(\phi_1+\pi G)^2+(\phi_2+\pi H)^2}{4t}\right)[1+(-1)^{G+K}] \times\left(\frac{2t-(\phi_1+\pi G)^2}{2t^2}-\frac{2t-(\phi_2+\pi H)^2}{4t^2}-\bar{l}_3{}^2\right). \quad (4.6)$$

The integrals in (4.6) are integrable analytically and can be expressed in terms of the modified Bessel functions of the second kind $K_n(x)$ with $n=$ half-odd integers, which can in turn be expressed as exponential functions of $\bar{l}_3$. Thus, using Eq. (4.4) and Eqs. (B5)–(B7) in Appendix B, we get

$$D_{xx}{}^{c(\kappa p;\kappa p)}(\phi_1\phi_2; l_3 l_3') =\frac{e^2}{M_\kappa r_0{}^3}\frac{\pi}{2} \times\sum_{m=-\infty}^{\infty}\sum_{n=-\infty}^{\infty}[1+(-1)^{m+n}]\frac{(\phi_1+\pi m)^2}{[(\phi_1+\pi m)^2(\phi+\pi n)^2]^{1/2}} \times\exp\{-|\bar{l}_3|[(\phi_1+\pi m)^2+(\phi_2+\pi n)^2]^{1/2}\}. \quad (4.7)$$

For nonzero $\bar{l}_3$, the sum in Eq. (4.7) converges very rapidly for general ϕ_1 and ϕ_2.

The remaining components of $D_{\alpha\beta}{}^{c(\kappa p;\kappa p)}(\phi_1\phi_2; l_3 l_3')$ can be expressed in similar forms and we list them in Appendix B [Eqs. (B9)–(B13)].

To obtain the sums over $\bar{l}_1$ and $\bar{l}_2$ with the restriction $\bar{l}_1+\bar{l}_2=$ odd integer, all that is necessary is to replace the factor $[1+(-1)^{m+n}]$ in Eqs. (4.7) and (B9)–(B13) by the factor $[(-1)^m+(-1)^n]$. Thus, for example, for the element $D_{xx}{}^{c(\kappa p;\kappa' p)}(\phi_1\phi_2; l_3 l_3')$ we obtain the result

$$D_{xx}{}^{c(\kappa p;\kappa' p)}(\phi_1\phi_2; l_3 l_3') =\frac{e_\kappa e_{\kappa'}}{(M_\kappa M_{\kappa'})^{1/2}r_0{}^3}\frac{\pi}{2}\sum_{m=-\infty}^{\infty}\sum_{n=-\infty}^{\infty}[(-1)^m+(-1)^n] \times\frac{(\phi_1+\pi m)^2}{[(\phi_1+\pi m)^2+(\phi_2+\pi n)^2]^{1/2}} \times\exp\{-|\bar{l}_3|[(\phi_1+\pi m)^2+(\phi_2+\pi n)^2]^{1/2}\}, \quad \kappa'\neq\kappa. \quad (4.8)$$

[12] J. K. Mackenzie, Ph.D. thesis, University of Bristol, 1949 (unpublished). This method is described in the paper by B. M. E. van der Hoff and G. C. Benson, Can. J. Phys. 31, 1087 (1953).

[13] M. J. Lighthill, *Introduction to Fourier Analysis and Generalized Functions* (Cambridge University Press, Cambridge, England, 1958).

It should be pointed out that when $|l_3|\gg 1$, and ϕ_1/π, ϕ_2/π are not small compared to 1, the dominant contribution to the sums in both Eqs. (4.7) and (4.8) is from the origin ($m=n=0$) terms. Thus, when these conditions are satisfied,

$$D_{xx}{}^{c(\kappa p;\kappa' p)}(\phi_1\phi_2;\, l_3 l_3')\simeq \frac{e_\kappa e_{\kappa'}}{(M_\kappa M_{\kappa'})^{1/2} r_0{}^3}\frac{\pi\phi_1{}^2}{(\phi_1{}^2+\phi_2{}^2)^{1/2}} \times\exp[-|\bar{l}_3|(\phi_1{}^2+\phi_2{}^2)^{1/2}],\quad \kappa\neq\kappa' \text{ or } \kappa\neq\kappa'. \quad (4.9)$$

The origin term given by Eq. (4.9) is exactly the expression obtained by Fuchs and Kliewer[4] for the lattice sums, where they replaced direct summation by an integral. However, when $|\bar{l}_3|$ is not large compared to unity and ϕ_1/π, ϕ_2/π are small compared to unity, the origin term no longer dominates the sums and this approximation method fails. This can easily be seen by comparing the magnitude of the origin term with that of the first nonzero term in either Eq. (4.7) or Eq. (4.8). Thus, for example, when we put $\phi_1=\phi_2=\phi$, Eq. (4.7) gives the relation

$$\frac{\text{(magnitude of origin term: } m=n=0)}{\text{(magnitude of 1st nonzero term: } m=n=1)} =\left|\frac{\phi}{\phi+\pi}\right|\exp(2^{1/2}|\bar{l}_3|\pi) =|(1+\pi/\phi)^{-1}|\exp(2^{1/2}|\bar{l}_3|\pi). \quad (4.9')$$

Hence, for a given $|\bar{l}_3|$, when ϕ is small such that the relation $|\pi/\phi|\simeq\exp(2^{1/2}|\bar{l}_3|\pi)$ holds, the approximation of using the origin term for the sums is no longer valid. In fact, for very-long-wavelength vibration modes, $\phi\to 0$ and the approximation method totally breaks down, since then the origin term approaches zero while the higher-order terms remain finite.

Equation (4.9) is a slowly varying function of $|\bar{l}_3|$ in certain regions of the Brillouin zone. For example, when $\phi_1=0.1$, $\phi_2=0$ and $|\bar{l}_3|\geq 2$, the origin term given by Eq. (4.9) is the dominating part of the sum. If we compare the magnitudes of $D_{xx}{}^{c(\kappa p;\kappa' p)}(\phi_1\phi_2;\, l_3 l_3')$ between a two-layer separation $|\bar{l}_3|=2$ and a ten-layer separation $|\bar{l}_3|=10$, we find that

$$\frac{|D_{xx}{}^{c(\kappa p;\kappa' p)}(0.1,\,0;\, l_3=1,\, l_3'=3)|}{|D_{xx}{}^{c(\kappa p;\kappa' p)}(0.1,\,0;\, l_3=1,\, l_3'=11)|}=e^{0.8}=2.225,$$

indicating a very slow drop of the the magnitude of sum with respect to layer-separation distance. When $|\bar{l}_3|=1$, we see from Eq. (4.9′) that the origin term does not dominate the sum, but nevertheless it contributes more than 50% to the sum's magnitude. In these regions where the Coulomb interactions between the layers drop off slowly, it is essential to include Coulomb interactions between all layers of the slab.

We now turn to the case when $l_3=l_3'$. Equation (4.7) and (B9)–(B13) are no longer useful since they become slowly convergent and we need to do the summing in a different manner. Consider first the case when $\kappa\neq\kappa'$, $p=p'$. In this case we have

$$D_{\alpha\beta}{}^{c(\kappa p;\kappa' p)}(\phi_1\phi_2;\, l_3 l_3) =\frac{e^2}{r_0{}^3(M_\kappa M_{\kappa'})^{1/2}}\sum_{\substack{\bar{l}_1\bar{l}_2\\ \bar{l}_1+\bar{l}_2=\text{odd}}}\frac{\exp(-i\bar{l}_1\phi_1-i\bar{l}_2\phi_2)}{(\bar{l}_1{}^2+\bar{l}_2{}^2)^{5/2}} \times[3\bar{l}_\alpha\bar{l}_\beta-\delta_{\alpha\beta}(\bar{l}_1{}^2+\bar{l}_2{}^2)]. \quad (4.10)$$

The restriction ($\bar{l}_1+\bar{l}_2=$ odd) implies that when $\bar{l}_1$ is odd, $\bar{l}_2$ must be even or vice versa. Hence, we can write

$$D_{xx}{}^{c(\kappa p;\kappa' p)}(\phi_1\phi_2;\, l_3 l_3) =\frac{e^2}{r_0{}^3(M_\kappa M_{\kappa'})^{1/2}}\frac{1}{\Gamma(\frac{5}{2})}(F_1+F_2), \quad (4.11)$$

where

$$F_1=\sum_{m=-\infty}^{\infty}\sum_{n=-\infty}^{\infty}\int_0^\infty dt\, t^{3/2} \times\exp[-4m^2t-2im\phi_1-4(n-\tfrac{1}{2})^2t-2i(n-\tfrac{1}{2})\phi_2] \times[8m^2-4(n-\tfrac{1}{2})^2], \quad (4.12a)$$

$$F_2=\sum_{m=-\infty}^{\infty}\sum_{n=-\infty}^{\infty}\int_0^\infty dt\, t^{3/2} \times\exp[-4(m-\tfrac{1}{2})^2t-2i(m-\tfrac{1}{2})\phi_1-4n^2t-2ni\phi_2] \times[8(m-\tfrac{1}{2})^2-4n^2]. \quad (4.12b)$$

Instead of transforming both the sums over m and n in Eqs. (4.12a) and (4.12b) by the Poisson's summation formula as we did for $\bar{l}_3\neq 0$, here we transform only the sum over m in Eq. (4.12a) and likewise only the sum over n in Eq. (4.12b). The first term in Eq. (4.12a) is

$$\sum_{m=-\infty}^{\infty}\sum_{n=-\infty}^{\infty}\int_0^\infty dt\, t^{3/2}\exp[-4m^2t-2im\phi_1-4(n-\tfrac{1}{2})^2t-2i(n-\tfrac{1}{2})\phi_2](8m^2) =\sum_{G=-\infty}^{\infty}\sum_{n=-\infty}^{\infty}\int_0^\infty dt\, t^{3/2}\exp[-4(n-\tfrac{1}{2})^2t-2i(n-\tfrac{1}{2})\phi_2]\left[\frac{2t-(\phi_1+\pi G)^2}{2t^2}\left(\frac{\pi}{4t}\right)^{1/2}e^{-(\phi_1+\pi G)^2/4t}\right] =\sum_{G=-\infty}^{\infty}\sum_{n=-\infty}^{\infty}\left(\frac{\pi}{4}\right)^{1/2}e^{-2i(n-1/2)\phi_2}\int_0^\infty dt e^{-at-b/t}\left[1-\frac{(\phi_1+\pi G)^2}{2t}\right], \quad (4.13)$$

where $a=4(n-\frac{1}{2})^2$ and $b=\frac{1}{4}(\phi_1+\pi G)^2$.

The integrals in (4.13) can be expressed in terms of $K_n(x)$ with n=integer [see Appendix B, Eq. (B8)]. Doing that and following the same procedure for the other terms in Eqs. (4.12a) and (4.12b), we can write Eq. (4.11) as

$$D_{xx}{}^{c(\kappa p;\kappa' p)}(\phi_1\phi_2;\, l_3l_3)=\frac{e^2}{r_0{}^3(M_\kappa M_{\kappa'})^{1/2}}\{\sum_{n=1}^{\infty}\sum_{m=-\infty}^{\infty}2\cos[(2n-1)\phi_1]$$
$$\times[(\pi m+\phi_2)^2K_0((2n-1)|\pi m+\phi_2|)+(|\pi m+\phi_2|/(2n-1))K_1((2n-1)|\pi m+\phi_2|)]$$
$$-\sum_{n=1}^{\infty}\sum_{m=-\infty}^{\infty}2\cos[(2n-1)\phi_2][(\pi m+\phi_1)^2K_0((2n-1)|\pi m+\phi_1|)]\},\quad(4.14)$$

where the sums of modified Bessel functions are very rapidly convergent.

The other components of $D_{\alpha\beta}{}^{c(\kappa p;\kappa' p)}(\phi_1\phi_2;\, l_3l_3)$ are listed in Appendix B, in Eqs. (B14)–(B17).

Finally, for the case when $\kappa=\kappa'$; $p=p'$, Eq. (2.9) gives

$$D_{\alpha\beta}{}^{c(\kappa p;\kappa p)}(\phi_1\phi_2;\, l_3l_3)=\frac{1}{M_\kappa}\sum_{\bar l_1+\bar l_2=\text{even}}^{\bar l_1,\bar l_2}\Phi_{\alpha\beta}{}^{c(\kappa p;\kappa p)}(\bar l_1\bar l_2;\, l_3l_3)\exp(-i\bar l_1\phi_1-i\bar l_2\phi_2)$$
$$=\frac{1}{M_\kappa}[\Phi_{\alpha\beta}{}^{c(\kappa p;\kappa p)}(00;\, l_3l_3)+\sum_{\bar l_1+\bar l_2=\text{even}}^{\bar l_1,\bar l_2{}'}\Phi_{\alpha\beta}{}^{c(\kappa p;\kappa p)}(\bar l_1\bar l_2;\, l_3l_3)\exp(-i\bar l_1\phi_1-i\bar l_2\phi_2)].\quad(4.15a)$$

The prime on the double sum indicates that the term $\bar l_1=\bar l_2=0$ is to be excluded. The first term $\Phi_{\alpha\beta}{}^{c(\kappa p;\kappa p)}(00;\, l_3l_3)$ is the atomic force tensor for the case $l_1=l_1'$, $l_2=l_2'$, and $l_3=l_3'$. This term can be found from the relation

$$\Phi_{\alpha\beta}{}^{c(\kappa p;\kappa p)}(00;\, l_3l_3)=-\sum_{\kappa' p'}\sum_{l_3'\bar l_1\bar l_2}{}'\Phi_{\alpha\beta}{}^{c(\kappa p;\kappa' p')}(\bar l_1\bar l_2;\, l_3l_3'),\quad(4.15b)$$

where the prime on the triple sum indicates that the point $\bar l_1=\bar l_2=0$, $l_3'=l_3$ is to be excluded. $\Phi_{\alpha\beta}{}^{c(\kappa p;\kappa p)}(00;\, l_3l_3)$ is equal to zero for a diatomic, infinitely extended crystal of cubic structure, but for our slab of finite number of layers, the elements which are diagonal in α and β are nonzero near the surfaces. We have listed in Table I the values of $\Phi_{\alpha\alpha}{}^{c(\kappa p;\kappa p)}(00;\, l_3l_3)$ as functions of l_3 for a slab with 15 layers.

We see that while $\Phi_{\alpha\alpha}{}^{c(\kappa p;\kappa p)}(00;\, l_3l_3)$ is negligible at a depth of three or four layers, its value at the surface is quite comparable to the other sums and hence cannot be neglected. Fuchs and Kliewer[4] have put these terms identically equal to zero in their treatment while Lucas[7] has included the surface term and neglected the rest.

The second term of Eq. (4.15a) is

$$D_{(2)\alpha\beta}{}^{c(\kappa p;\kappa p)}(\phi_1\phi_2;\, l_3l_3)=\frac{-e^2}{M_\kappa r_0{}^3}\sum_{\bar l_1+\bar l_2=\text{even}}^{\bar l_1,\bar l_2{}'}\frac{\exp(-i\bar l_1\phi_1-i\bar l_2\phi_2)}{(\bar l_1{}^2+\bar l_2{}^2)^{5/2}}[3\bar l_\alpha\bar l_\beta-\delta_{\alpha\beta}(\bar l_1{}^2+\bar l_2{}^2)].\quad(4.16)$$

By using the same method as used for the ($\bar l_1+\bar l_2$= odd) sums but taking care to exclude the point $\bar l_1=\bar l_2=0$ from the double sum, we express Eq. (4.16) in terms of rapidly convergent sums of modified Bessel functions. Thus, for example,

$$D_{(2)xx}{}^{c(\kappa p;\kappa p)}(\phi_1\phi_2;\, l_3l_3)=\frac{-e^2}{M_\kappa r_0{}^3}\Big\{\frac{4}{3}\Big(\sum_{n=1}^{\infty}\sum_{m=-\infty}^{\infty}\cos(2n\phi_1)\Big[(\pi m+\phi_2)^2K_0(2n|\pi m+\phi_2|)+\frac{|\pi m+\phi_2|}{n}K_1(2n|\pi m+\phi_2|)\Big]$$
$$-\sum_{n=1}^{\infty}\sum_{m=-\infty}^{\infty}\cos(2n\phi_2)\Big[\tfrac{1}{2}(\pi m+\phi_1)^2K_0(2n|\pi m+\phi_1|)+\frac{|\pi m+\phi_1|}{2n}K_1(2n|\pi m+\phi_1|)\Big]$$
$$+\sum_{n=1}^{\infty}\sum_{m=-\infty}^{\infty}(-1)^m\cos((2n-1)\phi_1)\Big[(\pi m+\phi_2)^2K_0((2n-1)|\pi m+\phi_2|)+\frac{2|\pi m+\phi_2|}{(2n-1)}K_1(|\pi m+\phi_2|(2n-1))\Big]$$
$$-\sum_{n=1}^{\infty}\sum_{m=-\infty}^{\infty}(-1)^m\cos[(2n-1)\phi_2]\Big[\tfrac{1}{2}(\pi m+\phi_1)^2K_0(|\pi m+\phi_1|(2n-1))+\frac{|\pi m+\phi_1|}{(2n-1)}K_1(|\pi m+\phi_1|(2n-1))\Big]\Big)\Big\}.\quad(4.17)$$

TABLE I. Matrix elements of $\Phi_\alpha{}^{c(\kappa p;\kappa p)}(00;l_3l_3)$ for a diatomic ionic crystal slab of 15 layers.

Layer number (l_3)	$\Phi_{xx}(00;l_3l_3)^{c(\kappa p;\kappa p)}=\Phi_{yy}(00;l_3l_3)^{c(\kappa p;\kappa p)}=-\frac{1}{2}\Phi_{zz}(00;l_3l_3)^{c(\kappa p;\kappa p)}$
1 or 15 (surface layers)	$e^2/r_0{}^3\times(-0.66147)$
2 or 14	$e^2/r_0{}^3\times(0.00763)$
3 or 13	$e^2/r_0{}^3\times(-0.00009)$
4 or 12	0

The other components are listed in Appendix B, in Eqs. (B18)–(B21).

V. NORMAL MODE FREQUENCIES OF AN IONIC CRYSTAL SLAB

In Secs. III and IV, we obtained the explicit forms of $D_{\alpha\beta}{}^{s(\kappa p;\kappa' p')}(\phi_1\phi_2;l_3l_3')$ and expressed the elements of $D_{\alpha\beta}{}^{c(\kappa p;\kappa' p')}(\phi_1\phi_2;l_3l_3')$ in terms of rapidly convergent sums which are easily evaluable for given values of l_3, l_3' and for arbitrary wave-vector components ϕ_1 and ϕ_2. The eigenvalue equation (2.6) is solved numerically for a crystal slab of 15 layers, where the physical quantities used were to fit a NaCl crystal. The physical constants on which these calculations were based are

$$M_+(\mathrm{Na})=38.16\times10^{-24}\ \mathrm{g/atom},$$
$$M_-(\mathrm{Cl})=58.85\times10^{24}\ \mathrm{g/atom},$$
$$r_0=2.814\times10^{-8}\ \mathrm{cm},\quad e=4.8\times10^{-10}\ \mathrm{esu},$$
$$A=9.288,\quad B=-1.165.$$

The 90 normal-mode frequencies $\{\omega_j(\phi_1,\phi_2)\}$ and the corresponding eigenvectors $\{\zeta_\alpha{}^{(j)(\kappa p)}(l_3)\}(j=1, 2, \cdots, 6N=90)$ were obtained for a mesh of values of $(\phi_1\phi_2)$ covering the irreducible element of the two-dimensional Brillouin zone (see Fig. 2). For a NaCl crystal slab of 15 layers, eight localized surfaces modes and 82 "bulk" vibrational modes are found. The optical "bulk" modes have a wide range of frequencies and their upper and lower bounds have frequencies at infinite wavelength shifted only slightly from the corresponding limiting LO and TO values of an infinitely extended crystal with cyclic boundary conditions (see Table II). Two Rayleigh-type waves with slightly different frequencies (the fractional frequency separation $\Delta\omega/\omega\simeq10^{-4}$) are found lying below the lower bound of the acoustic "bulk" modes (Fig. 3). For the optical modes, we find at $\phi_1=\phi_2=0$, two TO surface modes whose eigenvectors have opposite parities, and whose frequencies are nearly degenerate with each other ($\Delta\omega/\omega\simeq10^{-4}$) and they lie below the TO limiting frequency of the infinitely extended crystal (Fig. 4). The two surface modes have ionic displacement amplitudes that attenuate exponentially at $\phi_1=\phi_2=0$ (see Fig. 5). This agrees with the results obtained by Lucas.[7] However, we find that each of these two modes is doubly degenerate. This is what one expects since

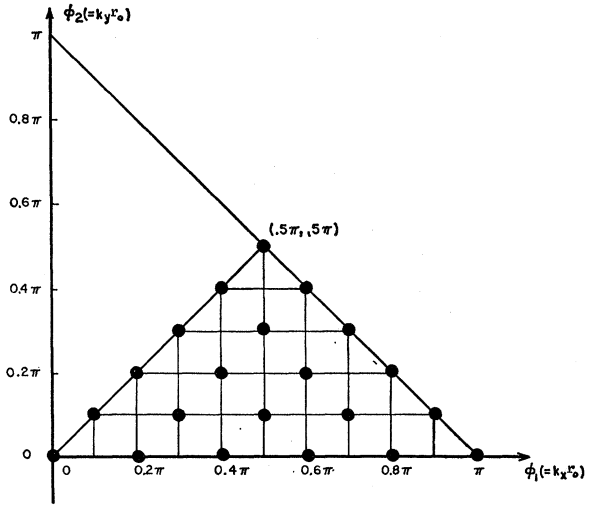

FIG. 2. Mesh of values for ϕ_1 and ϕ_2 chosen in the irreducible element of the two-dimensional first Brillouin zone. $\phi_1=\pi q_1/10$ and $\phi_2=\pi q_2/10$, where q_1 and q_2 are integers satisfying the relations $q_1\geq q_2$ and $q_1+q_2\leq10$.

these are transverse modes at $\phi_1=\phi_2=0$ and the ions vibrate either in the x direction or the y direction, both parallel to the surfaces. As we go away from the point $\phi_1=\phi_2=0$, we find two nearly degenerate higher-frequency surface modes ($\Delta\omega/\omega\simeq10^{-4}$) having exponentially decaying displacement amplitudes and they correspond to the higher-frequency surface optical mode found by Fuchs and Kliewer.[4] However, unlike their result, these two modes have limiting frequencies at infinite wavelength different from the LO limiting frequency of the infinitely extended crystal. The displacement amplitudes of these two upper-surface modes have very little attenuation at the point $\phi_1=\phi_2=0$ and at this point, their frequencies are no longer nearly degenerate ($\Delta\omega/\omega\simeq10^{-2}$). The fact that surface modes

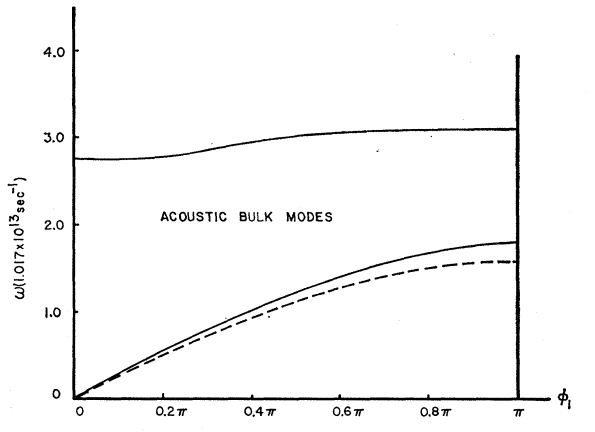

FIG. 3. Acoustic bulk modes and the Rayleigh waves propagating in the x direction ($\phi_2=0$) for a 15-layer NaCl crystal slab. The dashed curve represents two nearly degenerate Rayleigh waves. The acoustic "bulk" modes have a wide range of frequencies lying within the two solid lines, which mark their upper and lower bounds.

TABLE II. Values of the upper- and lower-bound frequencies at $\phi=0$ of the optical "bulk" modes for a 15-layer NaCl crystal slab and the limiting LO and TO frequencies of an infinitely extended crystal with cyclic boundary conditions ($\phi_1=\phi_2=0$).

Longitudinal optical mode	$\omega_{LO}(\text{Infinite crystal})=\left[\frac{e^2}{2r_0^3}\left(\frac{1}{M_+}+\frac{1}{M_-}\right)\left(A+2B+\frac{8\pi}{3}\right)\right]^{1/2}$	ω_{up}(unrelaxed)	% shift from ω_{LO}(infinite crystal)
	$A=9.288$, $B=-1.165$		
	5.852×10^{13} sec^{-1}	5.837×10^{-3} sec^{-1}	-0.26%
Transverse optical mode	$\omega_{TO}(\text{Infinite crystal})=\left[\frac{e^2}{2r_0^3}\left(\frac{1}{M_+}+\frac{1}{M_-}\right)\left(A+2B-\frac{4\pi}{3}\right)\right]^{1/2}$	ω_{low}(unrelaxed)	% shift from ω_{TO}(infinite crystal)
	$A=9.288$, $B=-1.165$		
	2.487×10^{13} sec^{-1}	2.491×10^{-13} sec^{1}	0.16%

comprise two branches, which are nearly degenerate in frequency, is due to the presence of two free surfaces and a plane of reflection symmetry midway between them. The surface modes in the presence of two free surfaces are essentially linear combinations of the surface modes associated with each of the surfaces separately of even and odd parity with respect to the midplane of the slab, and consequently they have slightly different frequencies. As the thickness of the slab is increased, the frequency of each of these surface modes approaches the frequency of a surface mode in a semi-infinite crystal.

VI. FREQUENCY SPECTRUM OF A SLAB

As was mentioned earlier in Sec. I, the method used here enables us to calculate the normal-mode frequencies of the slab for arbitrary wave-vector components in the two-dimensional Brillouin zone. Thus, it is possible to determine the frequency spectrum of the slab, which is required for many applications, and to compare it with that calculated for an infinite crystal. We divide the frequency scale into intervals of $\Delta\omega=0.3\times10^{13}$ sec^{-1}, and calculate the normal-mode frequencies for a NaCl crystal slab of 10 layers using 100 points in the two-dimensional first Brillouin zone. (This gives us a total of 6000 frequencies.) For the infinitely extended crystal we use the normal-mode frequencies calculated by Kellermann[11] for NaCl.[14] The results are shown in Fig. 6. In Fig. 7 the difference between the two frequency histograms is plotted and we find three maxima in the frequency intervals (1.2–1.5), (2.1–2.4), and (3.6–3.9)$\times10^{13}$ sec^{-1}. These maxima are due to the Rayleigh waves and to the optical surface waves. The peak at (2.1–2.4)$\times10^{13}$ sec^{-1} is much higher than the other two, and this is because the frequencies of the surface modes occurring in that interval are weakly dependent on the wave vectors. (See Fig. 4.)

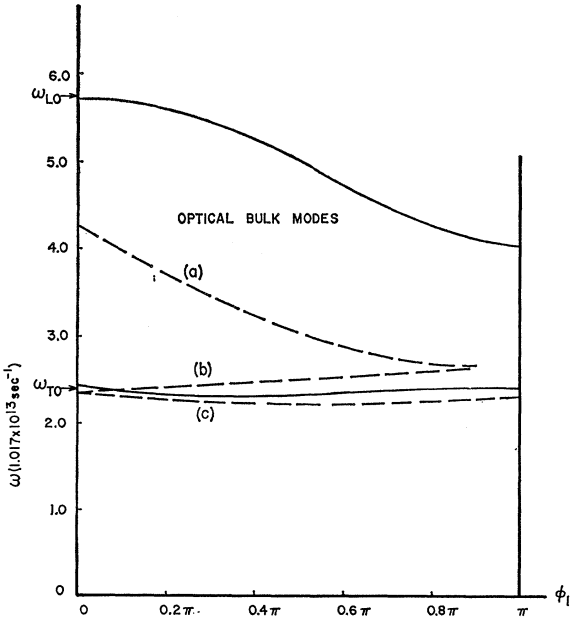

FIG. 4. Optical bulk modes and the optical surface modes propagating in the x direction ($\phi_2=0$) for a 15-layer NaCl crystal slab. Each of the three dashed curves marked (a), (b), and (c) represents two optical surface modes. The optical bulk modes have a wide range of frequencies lying within the two solid lines, which mark their upper and lower bounds.

VII. INFRARED LATTICE ABSORPTION OF AN IONIC CRYSTAL SLAB

One of the ways of detecting optical surface modes in an ionic crystal slab is by measuring the infrared absorption spectrum of the slab. Optical surface modes have a dipole moment associated with them, and should absorb electromagnetic radiation at the frequencies of these modes. Thus, one should observe peaks in the infrared absorption spectrum due to the surface optical modes at frequencies different from the bulk optical mode frequencies.

In this section, we calculate the imaginary part of the dielectric response tensor $\epsilon_{\mu\nu}^{(2)}(\omega)$, which has peaks at the same frequencies as the infrared absorption coefficient. The imaginary part of the dielectric re-

[14] In the result listed by Kellermann (Table IV) in his paper for the normal-mode frequencies of the infinite crystal, he included the point (10,5,0), which does not belong to the mesh of wave vectors he has chosen. Instead, the point (7,7,1), which should be included in the mesh, is missing.

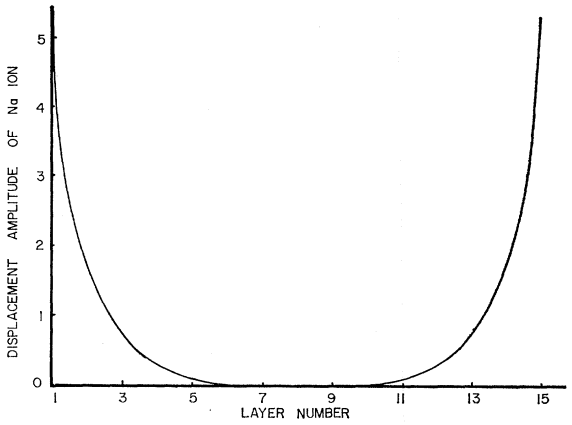

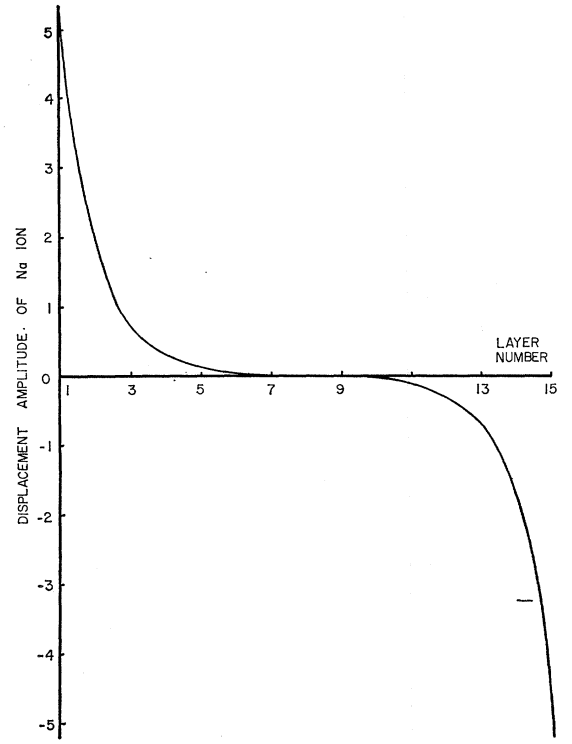

FIG. 5. Attenuation curve of the ionic displacement amplitude of the (+) ion for the TO surface modes of a 15-layer NaCl crystal slab at $\phi_1=\phi_2=0$. (a) and (b) shows the displacement amplitudes of the sodium ion plotted against the layer number for an even and an odd surface optical mode, respectively. Each of the even or odd mode is doubly degenerate; the displacement amplitude of the Na ion can either be in the x or y direction. A similar attenuation curve can be plotted for the displacement amplitude of the chlorine ion.

sponse tensor can be written in the form[15]

$$\epsilon_{\mu\nu}{}^{(2)}(\omega)=2\pi\left(\frac{e^{\beta\hbar\omega}-1}{\hbar V}\right)\int_0^\infty dt\, e^{-i\omega t}\langle M_\nu(t)M_\mu(0)\rangle, \quad (7.1)$$

[15] This result follows from Eq. (8.14) of the article by A. A. Maradudin, in *Astrophysics and the Many-Body Problem* (W. A. Benjamin, Inc., New York, 1963), p. 107, if the dielectric tensor is related to the dielectric susceptibility tensor by $\epsilon_{\mu\nu}(\omega)=\delta_{\mu\nu}+4\pi X_{\mu\nu}(\omega)$.

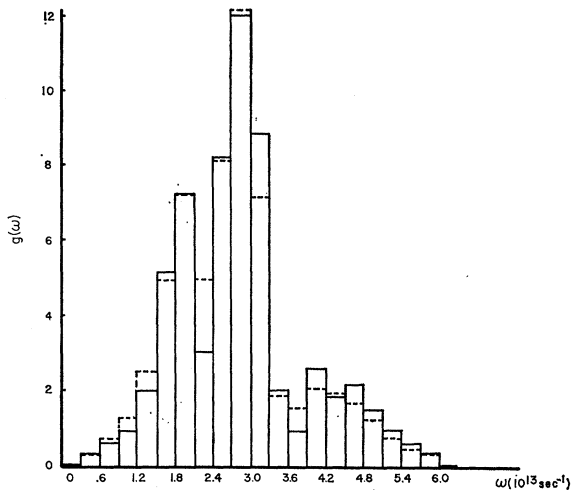

FIG. 6. Frequency-distribution histograms of a NaCl crystal slab of 10 layers and that of an infinite crystal. The histogram bounded by the dashed curve is for a slab of 10 layers while the one bounded by the solid curve is for an infinitely extended crystal.

where V is the volume of the crystal and $M_\mu(t)$ is the Heisenberg representation operator for the μ component of the crystal dipole moment. Writing $M_\mu(t)$ as

$$M_\mu(t)=\sum_{l\kappa} e_\kappa u_\mu(l\kappa;\, t), \quad (7.2)$$

Eq. (7.1) becomes

$$\epsilon_{\mu\nu}{}^{(2)}(\omega)=\frac{2\pi}{\hbar Vn(\omega)}\sum_{l\kappa;l'\kappa'}\frac{e_\kappa e_{\kappa'}}{(M_\kappa M_{\kappa'})^{1/2}}\times\int_0^\infty dt\, e^{-i\omega t}\langle V_\nu(l\kappa;\, t)V_\mu(l'\kappa';\, 0)\rangle$$

$$=\frac{2\pi}{\hbar Vn(\omega)}\sum_{l_1l_2l_3}\sum_{l_1'l_2'l_3'}\frac{e^2(-1)^{l_1+l_2+l_3}(-1)^{l_1'+l_2'+l_3'}}{[M(l_1l_2l_3)M(l_1'l_2'l_3')]^{1/2}}\times\int_0^\infty dt\, e^{-i\omega t}\langle V_\nu(l_1l_2l_3;\, t)V_\mu(l_1'l_2'l_3';\, 0)\rangle, \quad (7.3)$$

where we have put $n(\omega)=(e^{\beta\hbar\omega}-1)^{-1}$ and

$$u_\mu(l\kappa)=V_\mu(l\kappa)/M_\kappa{}^{1/2}.$$

We can apply a normal coordinate transformation on the displacement amplitudes $V_\mu(l_1l_2l_3;\, t)$ by putting

$$V_\mu(l_1l_2l_3;\, t)=\left(\frac{\hbar}{2L^2}\right)^{1/2}\sum_{\phi_1\phi_2}\sum_j\frac{\exp(il_1\phi_1+il_2\phi_2)}{[\omega_j(\phi_1\phi_2)]^{1/2}}\times\zeta_\mu{}^{(j)}(\phi_1\phi_2;\, l_3)A_j(\phi_1\phi_2;\, t), \quad (7.4)$$

where $\boldsymbol{\phi}=(\phi_1,\phi_2)$ sums over the two-dimensional first Brillouin zone and L^2 is the number of ions in each layer of the slab. For an ionic slab of N layers, the index $j(=1, 2, \cdots, 6N)$ labels the $6N$ normal-mode solutions of Eq. (2.6). The field operator $A_j(\boldsymbol{\phi};\, t)$ can be expressed in terms of the creation and destruction phonon

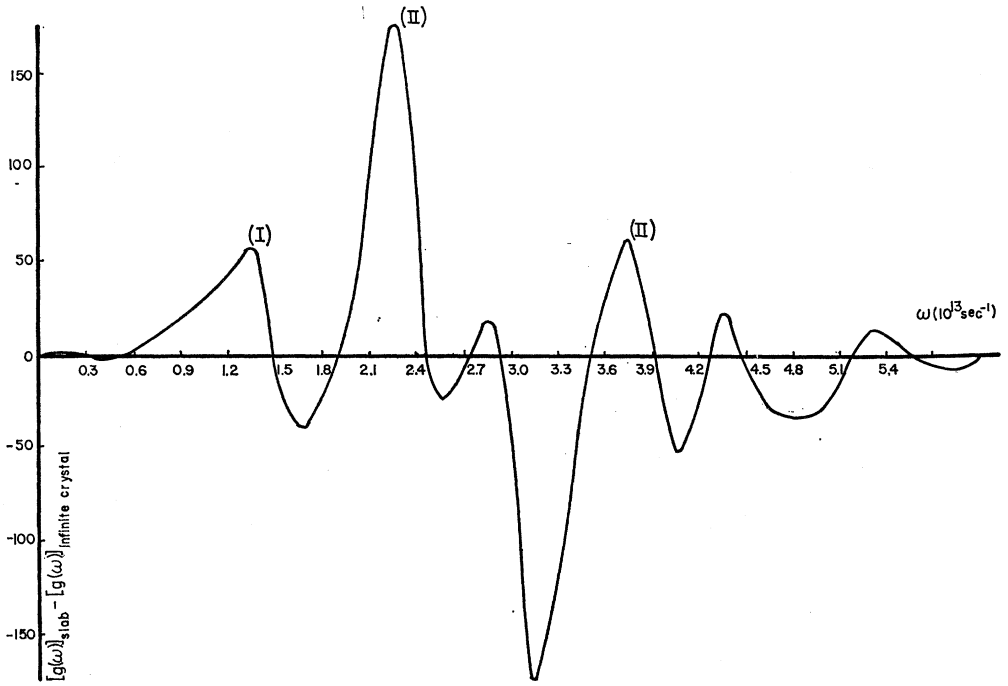

FIG. 7. Curve showing the difference between the frequency distribution of a NaCl crystal slab of 10 layers and that of an infinitely extended crystal.

operators for the mode $(\boldsymbol{\phi},j)$ as

$$A_j(\boldsymbol{\phi};t)=b_j(\boldsymbol{\phi})\exp[-i\omega j(\boldsymbol{\phi})t]+b_j^{\dagger}(-\boldsymbol{\phi})\exp[i\omega j(\boldsymbol{\phi})t]=A_j^{\dagger}(-\boldsymbol{\phi};t), \quad (7.5)$$

and the creation and destruction operators obey the following commutation relations:

$$\langle b_j(\boldsymbol{\phi})b_{j'}^{\dagger}(\boldsymbol{\phi}')\rangle=[n(\omega_j(\boldsymbol{\phi}))+1]\delta_{jj'}\delta_{\boldsymbol{\phi}\boldsymbol{\phi}'}, \quad (7.6a)$$

$$\langle b_j(\boldsymbol{\phi})b_{j'}(\boldsymbol{\phi}')\rangle=\langle b_j^{\dagger}(\boldsymbol{\phi})b_{j'}^{\dagger}(\boldsymbol{\phi}')\rangle=0, \quad (7.6b)$$

$$\langle b_j^{\dagger}(\boldsymbol{\phi})b_{j'}(\boldsymbol{\phi}')\rangle=n(\omega_j(\boldsymbol{\phi}))\delta_{jj'}\delta_{\boldsymbol{\phi}\boldsymbol{\phi}'}. \quad (7.6c)$$

The eigenvectors $\{\zeta_\mu^{(j)}(\phi_1\phi_2;l_3)\}$ are normalized by the relation

$$\sum_{l_3\mu}\zeta_\mu^{(j)}(\phi_1\phi_2;l_3)\zeta_\mu^{(j')*}(\phi_1\phi_2;l_3)=\delta_{jj'}. \quad (7.7)$$

Using Eqs. (7.4)–(7.6), we obtain from Eq. (7.3)

$$\epsilon_{\mu\nu}^{(2)}(\omega)=\frac{2\pi^2e^2}{VL^2}\sum_{\phi_1\phi_2}\sum_j\frac{\delta[\omega-\omega_j(\boldsymbol{\phi})]-\delta[\omega+\omega_j(\boldsymbol{\phi})]}{\omega_j(\boldsymbol{\phi})}\times\sum_{l_1l_2l_3}\sum_{l_1'l_2'l_3'}\frac{(-1)^{l_1+l_2+l_3}(-1)^{l_1'+l_2'+l_3'}}{[M(l_1l_2l_3)M(l_1'l_2'l_3')]^{1/2}}\times\exp[i(l_1-l_1')\phi_1+i(l_2-l_2')\phi_2]\times\zeta_\mu^{(j)}(\boldsymbol{\phi};l_3)\zeta_\nu^{*(j)}(\boldsymbol{\phi};l_3'). \quad (7.8)$$

The delta function $\delta[\omega+\omega_j(\boldsymbol{\phi})]$ is identically equal to zero if we restrict ourselves to the frequency region $\omega>0$. The triple sum over l_1, l_2, l_3 in Eq. (7.8) can be broken up in the following way:

$$\sum_{l_1l_2l_3}\frac{(-1)^{l_1+l_2+l_3}}{M(l_1l_2l_3)^{1/2}}\exp(il_1\phi_1+l_2\phi_2)\zeta_\mu^{(j)}(\boldsymbol{\phi};l_3)=\sum_{l_3}\sum_{\substack{l_1l_2\\ l_1+l_2=\text{even}}}\frac{\zeta_\mu^{(j)(+e)}(\boldsymbol{\phi};l_3)}{M_+^{1/2}}\exp(il_1\phi_1+il_2\phi_2)-\sum_{l_3}\sum_{\substack{l_1l_2\\ l_1+l_2=\text{odd}}}\frac{\zeta_\mu^{(j)(-e)}(\boldsymbol{\phi};l_3)}{M_-^{1/2}}\exp(il_1\phi_1+il_2\phi_2)+\sum_{l_3}\sum_{\substack{l_1l_2\\ l_1+l_2=\text{odd}}}\frac{\zeta_\mu^{(j)(+o)}}{M_+^{1/2}}\exp(il_1\phi_1+il_2\phi_2)-\sum_{l_3}\sum_{\substack{l_1l_2\\ l_1+l_2=\text{even}}}\frac{\zeta_\mu^{(j)(-o)}}{M_-^{1/2}}\exp(il_1\phi_1+il_2\phi_2). \quad (7.9)$$

The periodic boundary condition implies that

$$\sum_{\substack{l_1l_2\\ l_1+l_2=\text{even}}}\exp(il_1\phi_1+il_2\phi_2)=\tfrac{1}{4}L^2[1+(-1)^{n_1+n_2}]\delta_{\phi_1,n_1\pi}\delta_{\phi_2,n_2\pi} \quad (7.10a)$$

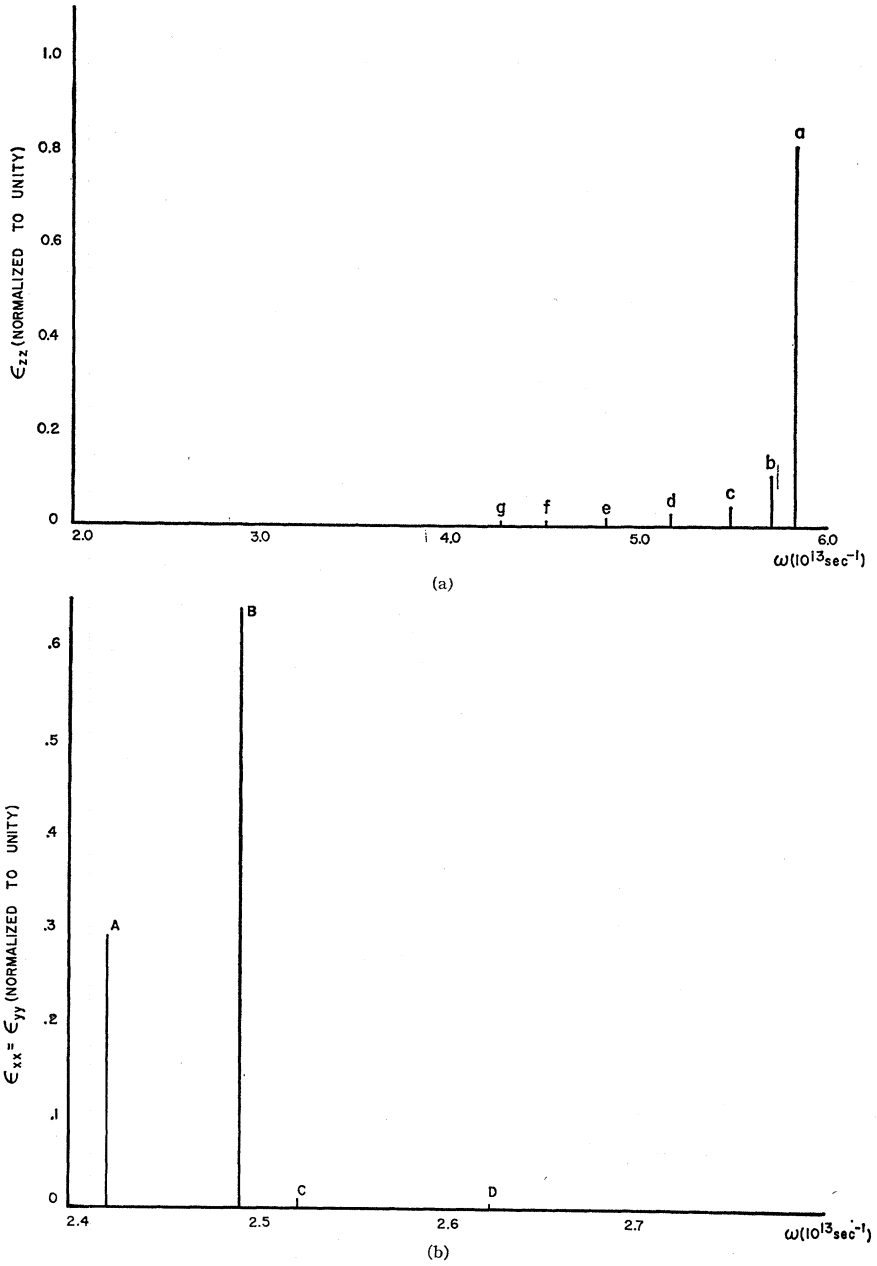

FIG. 8. Imaginary part of the crystal dielectric response tensor for a 15-layer NaCl crystal slab. $\epsilon_{zz}(\omega)$ in (a) and $\epsilon_{xx}(\omega)$ in (b) are normalized such that $\int_0^\infty \epsilon_{\mu\mu}(\omega)d\omega=1$.

and

$$\sum_{\substack{l_1 l_2 \\ l_1+l_2=\text{odd}}} \exp(il_1\phi_1+il_2\phi_2)=\tfrac{1}{4}L^2[(-1)^{n_1}+(-1)^{n_2}]\delta_{\phi_1,n_1\pi}\delta_{\phi_2,n_2\pi}, \tag{7.10b}$$

where $n_1,n_2=0, 1, 2\cdots\infty$. The wave vectors corresponding to $n_1+n_2=2n$ $(n=1, 2, \cdots\infty)$ are outside the two-dimensional first Brillouin zone and are equivalent to the point $\phi_1=\phi_2=0$ in the first Brillouin zone; hence, the dielectric tensor $\epsilon_{\mu\nu}{}^{(2)}(\omega)$ in Eq. (7.9) depends only on the normal modes at $\phi=0$. Using the relations given in Eqs. (7.10a) and (7.10b), we finally obtain

$$\epsilon_{\mu\nu}{}^{(2)}(\omega)=\frac{\pi^2e^2}{N(2r_0{}^3)}\sum_j \frac{\delta[\omega-\omega_j(0)]}{\omega_j(0)}\left(\sum_{l_3}\frac{\zeta_\mu{}^{(j)(+e)}(0;l_3)}{M_+{}^{1/2}}-\sum_{l_3}\frac{\zeta_\mu{}^{(j)(-e)}(0;l_3)}{M_-{}^{1/2}}+\sum_{l_3}\frac{\zeta_\mu{}^{(j)(+o)}(0;l_3)}{M_+{}^{1/2}}-\sum_{l_3}\frac{\zeta_\mu{}^{(j)(-o)}(0;l_3)}{M_-{}^{1/2}}\right)$$
$$\times\left(\sum_{l_3'}\frac{\zeta^{*(j)(+e)}(0;l_3')}{M_+{}^{1/2}}-\sum_{l_3'}\frac{\zeta_\nu{}^{*(j)(-e)}(0;l_3')}{M_-{}^{1/2}}+\sum_{l_3'}\frac{\zeta_\nu{}^{*(j)(+o)}(0;l_3')}{M_+{}^{1/2}}-\sum_{l_3'}\frac{\zeta_\nu{}^{*(j)(-o)}(0;l_3')}{M_-{}^{1/2}}\right). \tag{7.11}$$

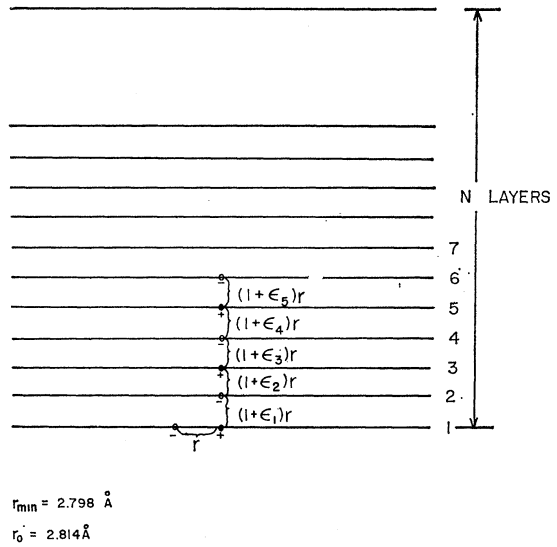

FIG. 9. Diatomic crystal slab of N layers with variable parameters $\epsilon_i (i=1, 2, \cdots, N-1)$ and r.

We have calculated the values of $\epsilon_{\mu\nu}{}^{(2)}(\omega)$ for a slab of 15 layers with M_+(=mass of sodium atom) and M_-(=mass of chlorine atom). At $\phi=0$, the tensor $\epsilon_{\mu\nu}{}^{(2)}(\omega)$ is diagonal in μ and ν and $\epsilon_{xx}{}^{(2)}(\omega)=\epsilon_{yy}{}^{(2)}(\omega)$. We show in Figs. 8(a) and 8(b) the values of $\epsilon_{zz}{}^{(2)}(\omega)$ and $\epsilon_{xx}{}^{(2)}(\omega)$, respectively, for different frequencies. Since the optical surface modes are transverse in nature at $\phi=0$, they only contribute to $\epsilon_{xx}{}^{(2)}(\omega)$. In Fig. 8(b), the line (A) at the lowest frequency is due to the TO surface modes while the lines (B), (C), and (D) at higher frequencies are due to the optical bulk modes. We see from this figure that, at least in the case of a slab of 15 layers, the absorption by the optical surface modes is comparable with that by bulk TO modes, and this result suggests that surface optical modes may be experimentally observable.

VIII. RELAXATION EFFECTS OF A SLAB

In the preceding sections we have assumed any two nearest-neighbor ions in the slab to be separated by a distance r_0 apart, where r_0 is taken to be the nearest-neighbor separation for an infinite crystal. As a consequence, the spacing between successive layers of the slab is restricted to be equal to r_0, so the layers (especially those near the surfaces) may not be at their true equilibrium positions. In this section, we vary the spacings between the layers and allow the interionic distance in each layer to change.[16] We then minimize the total potential energy of the slab as a function of the interionic distance and the separation distances of the layers, and estimate the magnitudes of the effects due to the relaxation on the surface modes.

[16] We assume the new interionic distance in each layer of the slab to be the same.

Let r be the separation distance between two adjacent ions in the same layer of a slab; then $r=r_0$ for an infinite crystal. Let the $(i+1)$th layer be separated from the ith layer by a distance $(1+\epsilon_i)r$, where ϵ_i is a parameter to be determined (see Fig. 9). Then the potential energy due to Coulomb interactions between the ith and $(i+n)$th layers (n=integer>0) is

$$V^c(i, i+n)=\frac{e^2}{r}L^2(-1)^n \times \sum_{l_1=-\infty}^{\infty}\sum_{l_2=-\infty}^{\infty}\left(\frac{(-1)^{l_1+l_2}}{[l_1^2+l_2^2+(n+\delta_n{}^i)^2]^{1/2}}\right), \quad (8.1)$$

where $\delta_n{}^i=\epsilon_i+\epsilon_{i+1}+\cdots+\epsilon_{i+n-1}$, and L^2 is the total number of ions in a layer.

We expand Eq. (8.1) in powers of $\delta_n{}^i$:

$$V^c(i, i+n)=\frac{e^2}{r}L^2(-1)^n\sum_{l_1=-\infty}^{\infty}\sum_{l_2=-\infty}^{\infty}(-1)^{l_1+l_2} \times\left[\frac{1}{(l_1^2+l_2^2+n^2)^{1/2}}-\delta_n{}^i\frac{n}{(l_1^2+l_2^2+n^2)^{3/2}} +\tfrac{1}{2}(\delta_n{}^i)^2\frac{(2n^2-l_1^2-l_2^2)}{(l_1^2+l_2^2+n^2)^{5/2}}+\cdots\right]$$
$$=(e^2/r)L^2\{(-1)^n[A(n)-\delta_n{}^iB(n)+(\delta_n{}^i)^2C(n)]\}, \quad (8.2)$$

where

$$A(n)=\sum_{l_1=-\infty}^{\infty}\sum_{l_2=-\infty}^{\infty}\frac{(-1)^{l_1+l_2}}{(l_1^2+l_2^2+n^2)^{1/2}}, \quad (8.3a)$$

$$B(n)=\sum_{l_1=-\infty}^{\infty}\sum_{l_2=-\infty}^{\infty}\frac{(-1)^{l_1+l_2}n}{(l_1^2+l_2^2+n^2)^{3/2}}, \quad (8.3b)$$

$$C(n)=\tfrac{1}{2}\sum_{l_1=-\infty}^{\infty}\sum_{l_2=-\infty}^{\infty}\frac{(-1)^{l_1+l_2}(2n^2-l_1^2-l_2^2)}{(l_1^2+l_2^2+n^2)^{5/2}}. \quad (8.3c)$$

In Eq. (8.2) we have kept terms in the expansion in powers of $\delta_n{}^i$ only up to the second order. This is because $(\delta_n{}^i)^\alpha\ll 1$ for $\alpha\geq 3$ and $n\leq 2$, while the coefficients of $(\delta_n{}^i)^\alpha$ become negligible for $n>2$. The sums $A(n)$, $B(n)$, and $C(n)$ are similar to those considered in Sec. IV, and can be expressed in terms of modified Bessel functions. They are listed in Appendix C.

Using Eq. (8.2), the total Coulomb energy due to interactions between all the layers of the slab is

$$\Phi^c(r;\epsilon_1,\cdots,\epsilon_{N-1}) =\frac{e^2}{r}[\sum_{i=1}^{N-1}\sum_{n=1}^{N-i}V^c(i, i+n)+N\Phi(0)]L^2, \quad (8.4)$$

where N is the number of layers in the slab, and

$$\Phi(0)=\tfrac{1}{2}\sum_{l_1,l_2}{}'\frac{(-1)^{l_1+l_2}}{(l_1^2+l_2^2)^{1/2}}$$

is the Coulomb interaction energy due to ions in the same layer. The prime on the double sum indicates that the term $l_1=l_2=0$ is to be excluded.

For the short-range interactions,

$$V^s(i,i+1)=L^2V(r(1+\epsilon_1))$$
$$=L^2[V(r)+\epsilon_i rV'(r)+\tfrac{1}{2}\epsilon_i^2r^2V''(r)+\cdots]$$
$$=\frac{e^2}{r}L^2[(rV(r)/e^2)+(\epsilon_i\tfrac{1}{4}B+\epsilon_i^2\tfrac{1}{8}A)], \quad (8.5)$$

where $V(r)$ is the short-range interaction potential between nearest-neighbor ions and we have made use of the constants A and B, defined in Eq. (3.1). Here, A and B are no longer constants but are functions of r and their functional forms depend on the explicit form of $V(r)$. For example, if we assume $V(r)$ to be the Born-Mayer potential $\lambda e^{-r/\rho}$, then

$$A=\frac{4r^3}{e^2}\left(\frac{\lambda}{\rho^2}\right)e^{-r/\rho}, \quad B=-\frac{4r^2}{e^2}\frac{\lambda}{\rho}e^{-r/\rho}.$$

The total short-range interaction potential energy for a slab of N layers is

$$\Phi^s(r;\epsilon_1,\cdots,\epsilon_{N-1})$$
$$=\frac{e^2}{r}L^2[(3N-1)\phi_0(r)+\sum_{i=1}^{N-1}(\tfrac{1}{4}B\epsilon_i+\tfrac{1}{8}A\epsilon_i^2)], \quad (8.6)$$

where $\phi_0(r)=(r/e^2)V(r)$. Adding Eqs. (8.4) and (8.6), we get the total potential energy,

$$\Phi^T(r;\epsilon_1,\cdots,\epsilon_{N-1})=\Phi^c(r;\epsilon_1,\cdots,\epsilon_{N-1})+\Phi^s(r;\epsilon_1,\cdots,\epsilon_{N-1}). \quad (8.7)$$

We minimize $\Phi^T(r;\epsilon_1,\cdots,\epsilon_{N-1})$ with respect to ϵ_i and r by solving the set of $N-1$ simultaneous equations

$$\frac{\partial\Phi^T}{\partial\epsilon_i}(r;\epsilon_1,\cdots,\epsilon_{N-1})=0, \quad i=1\cdots N-1$$

for different values of r. We then determine the value of $r_{\min}$ at which $\Phi^T(r;\epsilon_1,\cdots,\epsilon_{N-1})$ is a minimum. For a NaCl crystal slab of 15 layers, using the Born-Mayer potential function for $V(r)$, we find that the minimum value of $\Phi^T(r;\epsilon_1,\cdots,\epsilon_{N-1})$ occurs at $r=2.798\times10^{-8}$ cm (see Fig. 10), giving a change of 0.57% from the value of $r_0=2.814\times10^{-8}$ cm of the infinitely extended crystal. The shifts in the interplanar separation distances at minimum potential and at other values of r are listed in Table III. Using the results at minimum potential, the normal-mode frequencies of a relaxed slab of 15 layers are calculated. The number of Rayleigh and optical surface modes remains the same, but their frequencies and those of the bulk modes are shifted from the corresponding frequencies of a slab of 15 layers without relaxation (see Table IV).

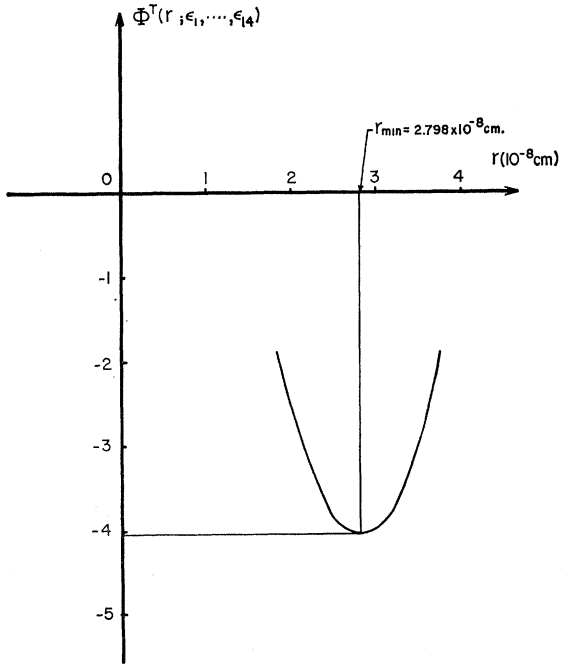

FIG. 10. Total potential energy of a 15-layer NaCl crystal slab as a function of the interionic separation distance r.

ACKNOWLEDGMENT

The first author wishes to thank Dr. D. L. Mills for his many helpful discussions during the course of this work.

TABLE III. Values of A, B, ϵ_i ($i=1, 2, \cdots, N-1$), and $\Phi^T(r;\epsilon_1,\cdots,\epsilon_{N-1})$ for different values of r for a 15-layer NaCl crystal slab with relaxation.

	$r(10^{-8}$ cm)	A	B	$\epsilon_1=\epsilon_{14}$	$\epsilon_2=\epsilon_{13}$	$\epsilon_3=\epsilon_{12}$	$\epsilon_4=\epsilon_{11}$	$\epsilon_5=\epsilon_{10}$	$\epsilon_6=\epsilon_9$	$\epsilon_7=\epsilon_8$	$\Phi^T(r,\epsilon_1,\cdots,\epsilon_{14})$
	2.818	9.223	−1.155	−0.0059	−0.0023	−0.0024	−0.0024	−0.0024	−0.0024	−0.0024	−4.06317
$r=r_0$(infinite crystal) →	2.814	9.288	−1.165	−0.0034	0.0001	0	0	0	0	0	−4.06329
	2.813	9.304	−1.167	−0.0028	0.0006	0.0005	0.0005	0.0005	0.0005	0.0005	−4.06332
$r=r_{\min}$ ⟶	2.798	9.547	−1.204	0.0059	0.0089	0.0088	0.0088	0.0088	0.0088	0.0088	−4.06351
	2.740	10.574	−1.362	0.0343	0.0361	0.0360	0.0360	0.0360	0.0360	0.0360	−4.05968
	2.700	11.332	−1.481	0.0496	0.0508	0.0508	0.0508	0.0508	0.0508	0.0508	−4.05153
	2.600	13.433	−1.823	0.0786	0.0791	0.0791	0.0791	0.0791	0.0791	0.0791	−4.00351

TABLE IV. Values of the upper- and lower-bound frequencies of the optical bulk modes and the frequencies of the optical surface modes and Rayleigh modes for a 15-layer NaCl crystal slab with and without relaxation. (a) is for the case when $\phi_1=\phi_2=0$ and (b) is for the case when $\phi_1=0.2\pi$ and $\phi_2=0$.

	Upper bound optical bulk mode ω_{up}	Lower bound optical bulk mode ω_{low}	Optical surface modes (a)	Optical surface modes (b)	Optical surface modes (c)	Rayleigh modes
			(A)			
15-layer slab (no relaxation) (10^{13} sec^{-1})	5.837	2.491	···	2.418	2.418	0 sec^{-1}
15-layer slab (with relaxation) (10^{13} sec^{-1})	5.944	2.561	···	2.516	2.516	0 sec^{-1}
Shifts of relaxed frequencies from unrelaxed frequencies (%)	1.83	2.81	···	4.05	4.05	0
			(B)			
15-layer slab (no relaxation) (10^{13} sec^{-1})	5.698	2.398	3.735	2.449	2.347	0.488
15-layer slab (with relaxation) (10^{13} sec^{-1})	5.750	2.503	3.783	2.547	2.456	0.486
Shifts of relaxed frequencies from unrelaxed frequencies (%)	0.91	4.37	1.28	4.0	4.64	−0.4

APPENDIX A: SHORT-RANGE FORCES WITH NEAREST- AND NEXT-NEAREST NEIGHBOR INTERACTIONS

$$D_{\alpha\beta}{}^{s(\kappa p;\kappa' p')}(\phi_1\phi_2;\, l_3 l_3') = \frac{1}{(M_\kappa M_{\kappa'})^{1/2}} \times \sum_{\bar{l}_1\bar{l}_2}{}^{(r)} \Phi_{\alpha\beta}{}^{s(\kappa p;\kappa' p')}(\bar{l}_1\bar{l}_2;\, l_3 l_3') \exp(-i\bar{l}_1\phi_1 - i\bar{l}_2\phi_2),$$
$$\kappa=(+) \text{ or } (-), \quad p=(e) \text{ or } (o). \quad \text{(A1)}$$

Let us define the following constants:

$$A=(4r_0{}^3/e^2)V'(r_0), \qquad B=(4r_0{}^2/e^2)V'(r_0),$$
$$A_1=(4r_0{}^3/e^2)V_1''(2^{1/2}r_0), \qquad B_1=(4r_0{}^2/2^{1/2}e^2)V_1'(2^{1/2}r_0),$$
$$A_2=(4r_0{}^3/e^2)V_2''(2^{1/2}r_0), \qquad B_2=(4r_0{}^2/2^{1/2}e^2)V_2'(2^{1/2}r_0),$$

where $V(r)$ = short-range interaction potential between nearest-neighbors ions, $V_1(r)$ = short-range interaction potential between next-nearest-neighbor (+) ions, $V_2(r)$ = short-range interaction potential between next-nearest-neighbor (−) ions, and the prime on each function denotes differentiation with respect to the respective arguments. The matrices $D_{\alpha\beta}{}^{s(\kappa p;\kappa' p')}(\phi_1\phi_2;\, l_3 l_3')$ are no longer all diagonal in form. We list the nonzero elements of the matrices below.

Case (i): $\kappa=\kappa=(+)$ ion, $p=p'$

If l_3 is not a surface layer, then

$$D_{xx}{}^{s(+p;+p)}(\phi_1\phi_2;\, l_3 l_3') = D_{yy}{}^{s(+p;+p)}(\phi_1\phi_2;\, l_3 l_3') = (e^2/r_0{}^3M_+)\delta_{l_3' l_3'} \times [\tfrac{1}{2}A+B+A_1+2B_1-\tfrac{1}{2}(A_1+B_1)\cos\phi_1\cos\phi_2],$$

$$D_{zz}{}^{s(+p;+p)}(\phi_1\phi_2;\, l_3 l_3') = (e^2/r_0{}^3M_+)\delta_{l_3,l_3'} \times [\tfrac{1}{2}A+B+A_1+2B_1-B_1\cos\phi_1\cos\phi_2],$$

$$D_{xy}{}^{s(+p;+p)}(\phi_1\phi_2;\, l_3 l_3') = (e^2/r_0{}^3M_+)\delta_{l_3,l_3}\tfrac{1}{2}(A_1-B_1)\sin\phi_1\sin\phi_2 = D_{yx}{}^{s(+p;+p)}(\phi_1\phi_2;\, l_3 l_3').$$

If l_3 is a surface layer, then

$$D_{xx}{}^{s(+p;+p)}(\phi_1\phi_2;\, l_3 l_3') = D_{yy}{}^{s(+p;+p)}(\phi_1\phi_2;\, l_3 l_3') = (e^2/r_0{}^3M_+)\delta_{l_3,l_3'} \times [\tfrac{1}{2}A+\tfrac{3}{4}B+\tfrac{3}{4}A_1+(5/4)B_1 - \tfrac{1}{2}(A_1+B_1)\cos\phi_1\cos\phi_2],$$

$$D_{zz}{}^{s(+p;+p)}(\phi_1\phi_2;\, l_3 l_3') = (e^2/r_0{}^3M_+)\delta_{l_3,l_3'} \times (\tfrac{1}{4}A+B+\tfrac{1}{2}A_1+\tfrac{3}{2}B_1-B_1\cos\phi_1\cos\phi_2),$$

$$D_{xy}{}^{s(+p;+p)}(\phi_1\phi_2;\, l_3 l_3') = (e^2/r_0{}^3M_+)\delta_{l_3,l_3'}\tfrac{1}{2}(A_1-B_1)\sin\phi_1\sin\phi_2 = D_{yx}{}^{s(+p;+p)}(\phi_1\phi_2;\, l_3 l_3').$$

For the case $\kappa=\kappa'=(-)$ ion, substitute A_2, B_2, and M_- for A_1, B_1, and M_+, respectively, in the above expressions.

Case (ii): $\kappa\neq\kappa'$, $p\neq p'$

The expressions for $D_{\alpha\beta}{}^{s(\kappa p;\kappa' p)}$ are exactly the same as those given in Eq. (3.4).

Case (iii): $\kappa=\kappa'=(+)$ ion, $p\neq p'$

$$D_{xx}{}^{s(+p;+p)}(\phi_1\phi_2;\, l_3l_3') = -(e^2/M_+r_0{}^3)[\tfrac{1}{4}(A_1+B_1)\cos\phi_1+\tfrac{1}{2}B_1\cos\phi_2] \times(\delta_{l_3,l_3'+1}+\delta_{l_3,l_3'-1}),$$

$$D_{yy}{}^{s(+p;+p')}(\phi_1\phi_2;\, l_3l_3') = -(e^2/M_+r_0{}^3)[\tfrac{1}{2}B_1\cos\phi_1+\tfrac{1}{4}(A_1+B_1)\cos\phi_2] \times(\delta_{l_3,l_3'+1}+\delta_{l_3,l_3'-1}),$$

$$D_{zz}{}^{s(+p;+p')}(\phi_1\phi_2;\, l_3l_3') = -(e^2/M_+r_0{}^3)[\tfrac{1}{4}(A_1+B_1)(\cos\phi_1+\cos\phi_2)] \times(\delta_{l_3,l_3'+1}+\delta_{l_3,l_3'-1}),$$

$$D_{xz}{}^{s(+p;+p')}(\phi_1\phi_2;\, l_3l_3') = -(e^2/M_+r_0{}^3)[i\tfrac{1}{4}(A_1-B_1)\sin\phi_1](\delta_{l_3,l_3'-1}-\delta_{l_3,l_3'+1}) = D_{zx}{}^{s(+p;+p')}(\phi_1\phi_2;\, l_3l_3'),$$

$$D_{yz}{}^{s(+p;+p')}(\phi_1\phi_2;\, l_3l_3') = -(e^2/M_+r_0{}^3)[i\tfrac{1}{4}(A_1-B_1)\sin\phi_2](\delta_{l_3,l_3'-1}-\delta_{l_3,l_3'+1}).$$

For the case $\kappa=\kappa'=(-)$ ion, substitute A_2, B_2, and M_- for A_1, B_1, and M_+, respectively, in the above expressions.

Case (iv): $\kappa\neq\kappa'$, $p\neq p'$

The expressions for $D_{\alpha\beta}{}^{s(\kappa p;\kappa' p')}(\phi_1\phi_2;\, l_3l_3')$ are the same as those given in Eq. (3.6).

APPENDIX B: ELEMENTS OF THE DYNAMICAL MATRIX FOR THE COULOMB INTERACTION

Using the Poisson's summation relations given in Eqs. (4.5c) and (4.5d), the following four summation rules are derived:

$$\sum_{m=-\infty}^{\infty} m^2 e^{-4m^2t-2im\phi} = \sum_{G=-\infty}^{\infty}\left(\frac{\pi}{4t}\right)^{1/2}\frac{2t-(\phi+\pi G)^2}{16t^2}e^{-(\phi+\pi G)^2/4t}, \tag{B1}$$

$$\sum_{m=-\infty}^{\infty}(m-\tfrac{1}{2})^2\exp[-4(m-\tfrac{1}{2})^2t-2i(m-\tfrac{1}{2})\phi] = \sum_{G=-\infty}^{\infty}(-1)^G\left(\frac{\pi}{4t}\right)^{1/2}\frac{2t-(\phi+\pi G)^2}{16t^2}e^{-(\phi+\pi G)^2/4t}, \tag{B2}$$

$$\sum_{m=-\infty}^{\infty} m e^{-4m^2t-2im\phi} = -i\sum_{G=-\infty}^{\infty}\frac{(\phi+\pi G)}{4t}\left(\frac{\pi}{4t}\right)^{1/2}e^{-(\phi+\pi G)^2/4t}, \tag{B3}$$

$$\sum_{m=-\infty}^{\infty}(m-\tfrac{1}{2})\exp[-4(m-\tfrac{1}{2})^2t-2i(m-\tfrac{1}{2})\phi] = -i\sum_{G=-\infty}^{\infty}(-1)^G\frac{(\phi+\pi G)}{4t}\left(\frac{\pi}{4t}\right)^{1/2}e^{-(\phi+\pi G)^2/4t}. \tag{B4}$$

Some useful integrals:

$$A=\int_0^\infty \frac{dt\, e^{-b^2t-a^2/4t}}{t^{1/2}} = \left(\frac{2|a|}{|b|}\right)^{1/2}K_{1/2}(|a||b|) = \frac{\pi^{1/2}}{|b|}e^{-|b||a|}, \quad |b|\neq 0 \tag{B5}$$

$$B=\int_0^\infty \frac{dt\, e^{-b^2t-a^2/4t}}{t^{3/2}} = \left(\frac{8|b|}{|a|}\right)^{1/2}K_{1/2}(|a||b|) = \frac{2\pi^{1/2}}{|a|}e^{-|b||a|}, \quad |a|\neq 0 \tag{B6}$$

$$C=\int_0^\infty dt\, e^{-b^2t-a^2/4t}t^{1/2} = 2\left(\frac{|a|}{2|b|}\right)^{3/2}K_{3/2}(|a||b_3|) = \tfrac{1}{2}\pi^{1/2}[(1+|a||b|)/|b|^3]e^{-|b||a|}, \quad |b|\neq 0 \tag{B7}$$

$$D=\int_0^\infty e^{-ax-b/x}\frac{dx}{x} = 2K_0(2(ab)^{1/2}), \quad a>0,\ b>0. \tag{B8}$$

The other components of $D_{\alpha\beta}{}^{c(\kappa p;\kappa p)}(\phi_1\phi_2;\, l_3l_3')$ for $|\tilde{l}_3|\neq 0$ are

$$D_{yy}{}^{c(\kappa p;\kappa p)}(\phi_1\phi_2;\, l_3l_3') = \frac{e^2}{M_\kappa r_0{}^3}\frac{\pi}{2}\sum_{m=-\infty}^{\infty}\sum_{n=-\infty}^{\infty}[1+(-1)^{m+n}] \times\frac{(\phi_2+\pi n)^2}{[(\phi_1+\pi m)^2+(\phi_2+\pi n)^2]^{1/2}}\exp\{-|\tilde{l}_3|[(\phi_1+\pi m)^2+(\phi_2+\pi n)^2]^{1/2}\}, \tag{B9}$$

$$D_{zz}^{c(\kappa p;\kappa p)}(\phi_1\phi_2;\, l_3 l_3') = -[D_{xx}^{c(\kappa p;\kappa p)}(\phi_1\phi_2;\, l_3 l_3') + D_{yy}^{c(\kappa p;\kappa p)}(\phi_1\phi_2;\, l_3 l_3')], \tag{B10}$$

$$D_{xy}^{c(\kappa p;\kappa p)}(\phi_1\phi_2;\, l_3 l_3') = \frac{e^2}{M_\kappa r_0^3}\frac{\pi}{2}\sum_{m=-\infty}^{\infty}\sum_{n=-\infty}^{\infty}[1+(-1)]^{m+n}\frac{(\phi_1+\pi m)(\phi_2+\pi n)}{[(\phi_1+\pi m)^2+(\phi_2+\pi m)^2]^{1/2}}$$
$$\times\exp\{-|\bar{l}_3|[(\phi_1+\pi m)^2+(\phi_2+\pi n)^2]^{1/2}\} = D_{yx}^{c(\kappa p;\kappa p)}(\phi_1\phi_2;\, l_3 l_3'), \tag{B11}$$

$$D_{xz}^{c(\kappa p;\kappa p)}(\phi_1\phi_2;\, l_3 l_3') = \frac{e^2}{M_\kappa r_0^3}\frac{\pi}{2}\sum_{m=-\infty}^{\infty}\sum_{n=-\infty}^{\infty}\frac{i\bar{l}_3}{|\bar{l}_3|}[1+(-1)^{m+n}](\phi_1+\pi m)$$
$$\times\exp\{-|\bar{l}_3|[(\phi_1+\pi m)^2+(\phi_2+\pi n)^2]^{1/2}\} = D_{zx}^{c(\kappa p;\kappa p)}(\phi_1\phi_2;\, l_3 l_3'), \tag{B12}$$

and

$$D_{yz}^{c(\kappa p;\kappa p)}(\phi_1\phi_2;\, l_3 l_3') = \frac{e^2}{M_\kappa r_0^3}\frac{\pi}{2}\sum_{m=-\infty}^{\infty}\sum_{n=-\infty}^{\infty}\frac{i\bar{l}_3}{|\bar{l}_3|}[1+(-1)^{m+n}](\phi_2+\pi n)$$
$$\times\exp\{-|\bar{l}_3|[(\phi_1+\pi m)^2+(\phi_2+\pi n)^2]^{1/2}\} = D_{zy}^{c(\kappa p;\kappa p)}(\phi_1\phi_2;\, l_3 l_3'). \tag{B13}$$

The other components of $D_{\alpha\beta}^{c(\kappa p;\kappa' p)}(\phi_1\phi_2;\, l_3 l_3)$ are

$$D_{yy}^{c(\kappa p;\kappa' p)}(\phi_1\phi_2;\, l_3 l_3) = \frac{e^2}{r_0^3(M_\kappa M_{\kappa'})^{1/2}}\Bigg\{\sum_{n=1}^{\infty}\sum_{m=-\infty}^{\infty}2\cos[(2n-1)\phi_2]$$
$$\times\left[(\pi m+\phi_1)^2 K_0((2n-1)|\pi m+\phi_1|)+\frac{|\pi m+\phi_1|}{(2n-1)}K_1((2n-1)|\pi m+\phi_1|)\right]$$
$$-\sum_{n=1}^{\infty}\sum_{m=-\infty}^{\infty}2\cos[(2n-1)\phi_1][(\pi m+\phi_2)^2 K_0((2n-1)|\pi m+\phi_2|)]\Bigg\}, \tag{B14}$$

$$D_{zz}^{c(\kappa p;\kappa' p)}(\phi_1\phi_2;\, l_3 l_3) = -[D_{xx}^{c(\kappa p;\kappa' p)}(\phi_1\phi_2;\, l_3 l_2) + D_{yy}^{c(\kappa p;\kappa' p)}(\phi_1\phi_2;\, l_3 l_3)], \tag{B15}$$

$$D_{xy}^{c(\kappa p;\kappa' p)}(\phi_1\phi_2;\, l_3 l_3) = -\frac{e^2}{r_0^3(M_\kappa M_{\kappa'})^{1/2}}\Bigg[\sum_{n=1}^{\infty}\sum_{m=-\infty}^{\infty}2(\pi m+\phi_1)|\pi m+\phi_1|\,\sin((2n-1)\phi_2)K_1((2n-1)|\pi_m+\phi_1|)$$
$$+\sum_{n=1}^{\infty}\sum_{m=-\infty}^{\infty}2(\pi m+\phi_2)|\pi m+\phi_2|\,\sin((2n-1)\phi_1)\,K_1((2n-1)|\pi m+\phi_2|)\Bigg] = D_{yx}^{c(\kappa p;\kappa' p)}(\phi_1\phi_2;\, l_3 l_3), \tag{B16}$$

and

$$D_{xz}^{c(\kappa p;\kappa' p)}(\phi_1\phi_2;\, l_3 l_3) = D_{yz}^{c(\kappa p;\kappa' p)}(\phi_1\phi_2;\, l_3 l_3) = D_{zx}^{c(\kappa p;\kappa' p)}(\phi_1\phi_2;\, l_3 l_3) = D_{zy}^{c(\kappa p;\kappa' p)}(\phi_1\phi_2;\, l_3 l_3) = 0. \tag{B17}$$

The other components of $D_{(2)\alpha\beta}^{c(\kappa p;\kappa p)}(\phi_1\phi_2;\, l_3 l_3)$ are

$$D_{(2)yy}^{c(\kappa p;\kappa p)}(\phi_1\phi_2;\, l_3 l_3)$$
$$= -\frac{e^2}{M_\kappa r_0^3}\frac{4}{3}\Bigg\{\sum_{n=1}^{\infty}\sum_{m=-\infty}^{\infty}\cos(2n\phi_2)\left[(\pi m+\phi_1)^2 K_0(2n|\pi m+\phi_1|)+\frac{|\pi m+\phi_1|}{n}K_1(2n|\pi m+\phi_1|)\right]$$
$$-\sum_{n=1}^{\infty}\sum_{m=-\infty}^{\infty}\cos(2n\phi_1)\left[\frac{(\pi m+\phi_2)^2}{2}K_0(2n|\pi m+\phi_2|)+\frac{|\pi m+\phi_2|}{2n}K_1(2n|\pi m+\phi_2|)\right]$$
$$+\sum_{n=1}^{\infty}\sum_{m=-\infty}^{\infty}(-1)^m\cos((2n-1)\phi_2)\left[(\pi m+\phi_1)^2 K_0((2n-1)|\pi m+\phi_1|)+\frac{2|\pi m+\phi_1|}{(2n-1)}K_1((2n-1)|\pi m+\phi_1|)\right]$$
$$-\sum_{n=1}^{\infty}\sum_{m=-\infty}^{\infty}(-1)^m\cos((2n-1)\phi_1)\left[\frac{(\pi m+\phi_2)^2}{2}K_0((2n-1)|\pi m+\phi_2|)+\frac{|\pi m+\phi_2|}{(2n-1)}K_1((2n-1)|\pi m+\phi_2|)\right], \tag{B18}$$

$$D_{(2)zz}{}^{c(\kappa p;\kappa p)}(\phi_1\phi_2;\, l_3l_3) = -[D_{(2)xx}{}^{c(\kappa p;\kappa p)}(\phi_1\phi_2;\, l_3l_3)+D_{(2)yy}{}^{c(\kappa p;\kappa p)}(\phi_1\phi_2;\, l_3l_3)], \tag{B19}$$

$$D_{(2)xy}{}^{c(\kappa p;\kappa p)}(\phi_1\phi_2;\, l_3l_3) = \frac{e^2}{M_\kappa r_0{}^3} 2\{\sum_{n=1}^{\infty}\sum_{m=-\infty}^{\infty}(\pi m+\phi_1)|\pi m+\phi_1|\,\sin(2n\phi_2)K_1(2n|\pi m+\phi_1|)$$

$$+\sum_{n=1}^{\infty}\sum_{m=-\infty}^{\infty}(-1)^m(\pi m+\phi_1)|\pi m+\phi_1|\,\sin[(2n-1)\phi_2]K_1((2n-1)|\pi m+\phi_1|)\} = D_{(2)yx}{}^{c(\kappa p;\kappa p)}(\phi_1\phi_2;\, l_3l_3), \tag{B20}$$

and

$$D_{(2)xz}{}^{c(\kappa p;\kappa p)}(\phi_1\phi_2;\, l_3l_3) = D_{(2)yz}{}^{c(\kappa p;\kappa p)}(\phi_1\phi_2;\, l_3l_3) = D_{(2)zx}{}^{c(\kappa p;\kappa p)}(\phi_1\phi_2;\, l_3l_3) = D_{(2)zy}{}^{c(\kappa p;\kappa p)}(\phi_1\phi_2;\, l_3l_3) = 0. \tag{B21}$$

APPENDIX C: EXPRESSIONS FOR $A(n)$, $B(n)$, $C(n)$, AND $\Phi(0)$ IN TERMS OF RAPIDLY CONVERGENT SUMS

$$A(n) = \sum_{l_1=1}^{\infty}\sum_{l_2=1}^{\infty}\frac{8}{((2l_1-1)^2+(2l_2-1)^2)^{1/2}}\exp\{-\pi|n|[(2l_1-1)^2+(2l_2-1)^2]^{1/2}\}, \tag{C1}$$

$$B(n) = \sum_{l_1=1}^{\infty}\sum_{l_2=1}^{\infty}8\pi\exp\{-\pi|n|[(2l_1-1)^2+(2l_2-1)^2]^{1/2}\}, \tag{C2}$$

$$C(n) = \sum_{l_1=1}^{\infty}\sum_{l_2=1}^{\infty}4\pi^2[(2l_1-1)^2+(2l_2-1)^2]^{1/2}\exp\{-\pi|n|[(2l_1-1)^2+(2l_2-1)^2]^{1/2}\}, \tag{C3}$$

$$\Phi(0) = \tfrac{1}{2}\sum_{l_1,l_2}{}'\frac{(-1)^{l_1+l_2}}{(l_1{}^2+l_2{}^2)^{1/2}} = \sum_{l_1=1}^{\infty}\sum_{l_2=1}^{\infty}4(-1)^{l_1}K_0(\pi l_1(2l_2-1))-\ln_e 2. \tag{C4}$$